國 立 交 通 大 學

環 境 工 程 研 究 所

碩 士 論 文

在配水管網中餘氯傳輸模式之研究

The Study of Model for Chlorine Transport in the Water Distribution System

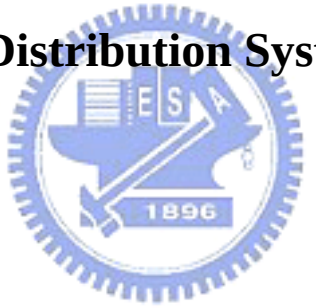

研究生：溫士賓

指導教授：葉弘德

中 華 民 國 九 十 七 年 九 月

在配水管網中餘氯傳輸模式之研究

The Study of Model for Chlorine Transport in the Water Distribution System

研究生：溫士賓　　Student: Shi-Bin Wen

指導教授：葉弘德　　Advisor: Hund-Der Yeh

國立交通大學

環境工程研究所

碩士論文

A Thesis
Submittd to Institute of Environmental Engineering
College of Engineering
National Chiao Tung University
in Partial Fulfillment of the Requirements
for the Degree of
Master of Science
in
Environmental Engineering
September, 2008
Hsinchu, Taiwan

中 華 民 國 九 十 七 年 九 月

致謝

在兩年的研究所生涯，即將劃下句點。回首這兩年的歲月，真的可以說是有歡笑有淚水，並且要感謝許多人的支持與幫助，才能順利完成學業。

首先，最先要感謝的人就是我的指導老師葉弘德教授，老師是一位學識豐富且研究認真的一位學者，他不僅細心教導我如何做研究，更讓我學到一些處事的態度，時間管理與執著努力為成功的不二法門，實在讓我受益良多。此外，也要特別感謝中興大學盧重興教授、中國科技大學陳主惠教授及台灣大學劉振宇教授擔任本論文的口試委員，在他們細心指正本論文一些疏失之處及提供許多寶貴意見，使本論文得以更加完整。

研究室裡有親切的學長姐們，他們從不吝嗇於提供他們寶貴的經驗與學弟妹分享，再加上熱心的學弟妹們，研究室就像是一個大家庭。由衷感謝雅琪學姊不厭其煩的解決我研究上的問題，並且細心的修改我的論文，是我研究順利的大推手，使我能夠在一年級的時候就有一些研究成果。而研究室成員，紹洋學長、智澤學長、彥禎學長、雅琪學姊、彥如學姊、嘉真學姊、志添學長、毓婷學姊、敏筠學姊、凱如學姊，他們都是我的好榜樣，從他們身上學到很多寶貴的知識與經驗，非常感謝他們在兩年來的照顧與指導。也謝謝珧儀、其珊、仲豪、庚轅及璟勝的協助，還有與我一同進入地下水研究室的博傑同學，我們經常分享研究與生活上的心得，謝謝他這兩年的幫助，也很高興能與他一起畢業。感謝環工所壘球隊的大家，我很高興能與你們一起打球、一起奮鬥，讓我兩年的生活更加多彩多姿。還有感謝楚俊、毅豪、家驤、詔元及燦煌你們的陪伴，使研究生活不再枯燥。

最後，深深地感謝我的家人，尤其是我的祖母、父母及兩位哥哥，你們給我的無條件的支持與關心，是讓我繼續走下去的動力，讓我能無後顧之憂地完成學業，在此送上我最由衷的謝意，謝謝你們。

在配水管網中餘氯傳輸及模式之研究

研究生：溫士賓　　指導教授：葉弘德

國立交通大學環境工程研究所

摘要

在配水管網中，餘氯的殘留關係到飲用水的安全。二維非穩態氯傳輸方程式可以描述餘氯在管中傳輸行為，此方程式考慮氯在軸向的傳流及延散作用，徑向的擴散作用和發生在水體及管壁上的一階消耗反應。目前已有許多數值模式被發展來模擬管網中餘氯的濃度，然而，在這個領域中解析解的研究是相當的稀少。本論文首先利用拉式轉換和廣義傅立葉級數展開推倒出在紊流中二維非穩態氯傳輸方程式的解析解，並且結合忽略軸向延散作用的解析解，及一系列數學方法，發展出可模擬管網中餘氯濃度的解析模式。此模式以美國康乃狄克州部份供水區域 (South Central Connecticut Regional Water Authority) 進行實際模擬配水管網中的餘氯濃度，結果將與一維質量傳輸模式 (*Rossman et al., 1994*) 比較。此外，本論文亦發展在紊流中穩態氯傳輸方程式的近似解。相較於 *Biswas et al.* (*1993*) 提出的近似解，此近似解具有容易計算與精度高的優點，並且可結合模擬退火演算法，發展出可以預測管壁消耗參數的方法。兩個案例研究驗證此近似解和數學方法的應用性。第一個案例是利用近似解模擬 *Rossman* (*2006*) 的餘氯消耗實驗結果，而另一案例為美國康乃狄克州部份供水區域(South Central Connecticut Regional Water Authority)中管壁消耗反應常數的預估結果。

關鍵字：解析解、近似解、 餘氯、管、配水系統、傳輸方程式、管壁消耗

The Study of Model for Chlorine Transport in the Water Distribution System

Student: Shi-Bin Wen Advisor: Hun-Der Yeh

Institute of Environmental Engineering

National Chiao Tung University

ABSTRACT

The residual chlorine concentration in a water distribution system concerns safety of drinking water. A mathematical model can be used to describe the transport behavior for chlorine in a pipe. This model is mainly make up of two dimension chlorine transport equation (CTE) considering the mechanisms of advection and dispersion in axial direction, the diffusion in radial direction, and the first-order decay reactions in the bulk liquid phase and at pipe wall. Many numerical techniques were utilized to solve the 1-D model and only few studies have been devoted to the development of analytical solution in this area. This study first derives the analytical solution of unsteady CTE in turbulent flow through utilization of Laplace transform and generalized Fourier series expansion, which is to simplify differential term in the radial direction. This solution is further simplified in absence of dispersion in axial direction and integrates with a series of methodology to establish an analytical model for simulating the chlorine residual at any location in a water network. This analytical model is used to predict the chlorine concentration distribution in the water network of the South Central Connecticut Regional Water Authority (SCCRWA). The simulated results are compared with those obtained from a mass-transfer-based model

developed by *Rossman et al.* (*1994*). Moreover, an approximate solution of the 2-D steady-state chlorine transport equation under turbulent flow is also developed. This new approximate solution has advantages of easy evaluation and good accuracy when compared with *Biswas et al.*'s approximate solution (*1993*). This thesis also develops a methodology which combines simulated annealing (SA) with this new approximate solution to determine the wall decay parameter. Two cases are chosen to demonstrate the application of the present approximate solution and methodology. The first case is to use this new approximate solution in simulating chlorine decay in pipes with the experiment-observed data given by *Rossman* (*2006*) while the second case presents the determination of the wall consumption at the end of pipe in the water network of SCCRWA.

KEY WORDS: analytical solution, approximate solution, chlorine, pipes, water distribution system, transport equation, wall decay.

TABLE OF CONTENTS

LIST OF TABLES

LIST OF FIGURES

NOTATION

C Point value of chlorine concentration in the any location of the pipe (mgl^{-1});

C' Average chlorine concentration in the pipe under no wall consumption Condition(mgl^{-1});

$\overline{C}$ Concentration in Laplace domain

C_{av} Cup-mixing average concentration of the pipe at any cross-section (mgl^{-1});

C_{avj}^{m} Cup-mixing average concentration at X_j within pipe j at mth hydraulic time step

$C_{initiali,j}^{m}$ Spatial concentration distribution of ith segment in pipe j at the beginning of the mth hydraulic time step (mgl^{-1});

C_m Well mixed concentration (mgl^{-1});

$C_{in\,j}$ The concentration at the inlet node of pipe j

C_{inlet} Inlet temporal concentration variable (mgl^{-1});

$C_{out\,j}$ The concentration at the out node of pipe j

$C_{initial}$ Initial spatial concentration distribution (mgl^{-1});

D Dimensionless chlorine radial diffusivity ($LD_r/r_0 2u$);

D_{eddy} Eddy diffusivity (m^2s^{-1});

D_r Radial effective diffusivity of chlorine in the water (m^2s^{-1});

D_x Axial effective diffusivities of chlorine in the water ($m^2\ s^{-1}$);

$f(r)$ Flow parameter term on the flow regime;

g Number of confluent node;

G Number of flow path;

J_0 Bessel function of the first kind of order zero;

J_1 Bessel function of the first kind of order one;

k_d First-order chlorine decay rate constant in the bulk water (s^{-1});

k_f mass transfer coefficient (ms^{-1})

K Dimensionless chlorine decay rate in the bulk water (k_dL/u);

L Pipe length (m);

m Number of hydraulic time step;

N Number of the last segment in pipe j;

P_L Dimensionless chlorine axial diffusivity (LU/D_x);

PT_j^m Retention time for water flow in pipe j at the mth hydraulic time step;

q_i Flow rate at confluent node i in a single flow path;

Q_i Total flow rate at confluent node i;

r_0 Pipe radius (m);

r_h Hydraulic radius of pipe;

R Dimensionless radial distance from the center of the pipe (r/r_0);

s Laplace parameter related to dimension time

$ST_{i,j}^m$ Retention times of ith segment in pipe j at the mth hydraulic time step;

t Time (s)

t_h Time of hydraulic time step (hr);

t_s Time of water quality time step (min);

T Dimensionless time (tu/L)

T_j^m Dimensionless time of pipe j at the mth hydraulic time step;

$T_j'^m$ Dimensionless time at the end of the mth HTS in pipe j,

u Average flow velocity throughout the distribution system (ms^{-1});

u_j^m Average flow velocities in pipe j at the mth hydraulic time step;

w_d Pipe wall surface reaction constant (ms^{-1});

W Dimensionless wall decay rate ($w_d r_0/D_r$);

x Axial distance from the inlet along the pipe (m);

X Dimensionless axial distance from the inlet along the pipe (x/L);

X_j Dimensionless axial location in pipe j ;

$\hat{\alpha}$ Dimensionless reaction parameter for initial condition;

$\tilde{\alpha}$ Dimensionless reaction parameter for inlet condition;

$\hat{\alpha}_{i,j}^{m}$ Dimensionless reaction parameter for ith segment in pipe j at mth hydraulic time step;

$\hat{\beta}$ Concentration parameter for initial condition (mgl^{-1});

$\tilde{\beta}$ Concentration parameter for inlet condition (mgl^{-1});

$\hat{\beta}_{i,j}^{m}$ Concentration parameter for ith segment in pipe j at the mth hydraulic time step;

ε Fractional error;

λ_n The nth root of Eq. (16);

τ Time within a hydraulic time step ($0 \sim t_h$).

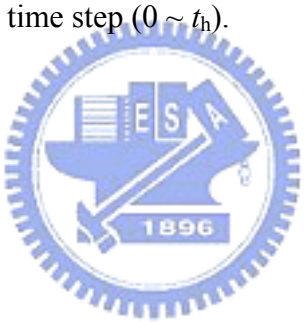

CHAPTER 1 INTRODUCTION

1.1 Background

The establishment of maximum contaminant level goals for some pernicious materials existing in the treated water after leaving from treatment plants was regulated by the Safe Drinking Water Act and its Amendments in US. More interest in water quality aggravation in the water distribution systems is by virtue of this command. In general, disinfection is carried out to reduce or prevent microbiological growth before treated water entering the water network system. Chlorine is a strong and enduring disinfectant which can control microbial growth in the distribution networks. When chlorine is added to water, it can combine with water rapidly to form hypochlorous acid (HOCl) and hydrochloric acid (HCl). Partial hypochlorous acid then ionizes to form the hydrogen ion (H^+) and the hypochlorite ion (OCl^-). The HOCl and OCl^- are called free available chlorine which has a strong disinfection capacity because it is a strong oxidizing agent capable of oxidizing substance in water, inclusive of microbe. Chlorine can react with the organic matters in water; however, the process may result in some carcinogens by-products, e.g., trihalomethanes (*Tchobanoglous and Schroeder*, *1987*). The quantity of residual chlorine should be small to avoid producing the carcinogens disinfection; however, there is no disinfection capacity in water if the concentration of residual chlorine is low. Consequently, it is very important to control the concentration of residual chlorine in water.

The model for chlorine transport in the pipes may include the first-order decay kinetics in bulk liquid and chlorine consumption at the pipe wall. The consumption process at the pipe wall is similar to the process of mass transfer from the bulk liquid phase to the pipe surface. *LeChevallier et al.* (*1988*) indicated that the transport of chlorine from the bulk liquid phase to the biofilm at the pipe wall is an important factor affecting the chlorine decay rate. In order to inactivate bacterial populations, higher chlorine concentrations are required

in the biofilm as compared to those suspended in the bulk liquid phase. In addition, the pipe material strongly affects the wall decay and could generally be grouped into two different types. That is the reactive pipes such as unlined iron and unreactive pipes, e.g., PVC, MDPE, cement-lined iron (*Hallam et al.*, *2002*). Additionally, pipe age also affect the capacity of chlorine reaction at the pipe wall (*Al-Jasser*, *2006*). Therefore, the decay of chlorine at the pipe wall is usually considered as the first order reaction parameter in relation to the degree of reactivity of the pipe material or growth of biofilm on the pipe wall.

1.2 Literature review

In the water distribution systems, minimum chlorine residual is required to ensure safe drinking water. Nevertheless, maintenance of this requirement is difficult due to chlorine decay with time comprising reactions in the bulk water and at the pipe wall. In order to realize the chlorine disappearance and transport behavior in pipes, an unsteady two dimensional (2-D) mathematical model is developed. The model is mainly composed of a chlorine transport equation (CTE) accounting for the processes of the advection and dispersion in axial direction, the diffusion in radial direction, and the decay with a first-order reaction in the bulk flow and at the pipe wall. *Biswas et al.* (*1993*) derived an analytical solution for a steady-state 2-D CTE without considering the axial dispersion under turbulent flow. Their analytical solution was further simplified to a simple exponential function form which can be easily applied to estimate chlorine decay or transport parameters in water networks. However, the development of the approximate solution is not straightforward and the accuracy of approximate solution may be influenced due to regression when the wall decay parameter is large. For the numerical approach, *Ozdemir* and *Ger* (*1998*) applied finite difference method to solve steady-state chlorine transport equation and simulated chlorine transport behavior in an experimental pipe. Alternating Direction Implicit (ADI) scheme was utilized to solve the unsteady 2-D CTE (*Ozdemir and Ger*, *1999*)

Previous studies on water quality in the water distribution systems included the development of the contaminant propagation model or the simulation of chlorine decay in the pipe network (e.g., *Clark et al.*, *1991*; *Clark et al.*, *1993*; *Clark et al.*, *1994*). Based on mass conservation, *Rossman et al.* (*1994*) developed an one dimensional (1-D) mass-transfer-based model with considering the advection in axial direction and introducing the concept of mass-transfer coefficient in representing chlorine transfer from bulk flow to the wall pipe. They integrated the mass-transfer-based model with the hydraulic model of EPANET to perform hydraulic and residual chlorine concentration simulations in the water networks (*Rossman et al.*, *1994*). The same model was also utilized for the determination of decay parameters in real networks by coupled with an optimization approach or statistical technique (e.g., *Vasconcelos et al.*, *1997*; *Munavalli1 and M. S. Kumar*, *2006*). *Munavalli* and *M. S. Kumar* (*2004a*) developed the relation of chlorine reaction to the substrate and microorganisms in water distribution systems based on a 1-D multi-component reaction transport model. Many numerical techniques were utilized to solve the 1-D model (e.g., *Rossman and Boulos*, 1993; *Rossman et al.*, *1996*; *Munavalli and M. S. Kumar*, *2004b*) and only few studies have been devoted to the development of analytical solution in this area. However, most of numerical techniques involve the problems of numerical dispersion and/or phase shift errors (*Rossman et al.*, *1996*; *Yeh*, *2000*).

1.3 Objectives

This study has two primary objectives. The first is to derive the closed form solutions of unsteady 2-D CTE with and without dispersion in turbulent flow using Laplace transform and technique of generalized Fourier series expansion. The closed form solution without axial dispersion is further utilized to develop an analytical model for simulating the chlorine concentration distribution in a water network based on the pipe velocities obtained from a hydraulic simulation. This model is applied to the simulation of the chlorine concentration in a water distribution system build by South Central Connecticut Regional Water Authority

(SCCRWA) for tracking the change of chlorine residual with time. The results of the present model will compare with the observed data and the predicted concentration by the mass-transfer-based model developed by *Rossman et al.* (*1994*). The second is to develop a new approximate solution of *Biswas et al.*'s analytical solution (*1993*) which has advantages of simple function form, easy numerical evaluation, and good accuracy. The approximate solution is obtained mainly by remaining the first term of the infinite series in the analytical solution of *Biswas et al.* (*1993*) and simplifying the Bessel function in eigenfunction. This approximate solution is expressed as an exponential form and in terms of three non-dimensional parameters, which physically represent the mechanisms of radial diffusion, first-order chlorine bulk decay, and chlorine wall decay. Thus, this approximate solution can be used to estimate transport parameters if coupled with an optimization algorithm. The two cases including experimental study (*Rossman*, *2006*) and study in the water network of SCCRWA (*Biswas et al.*, *1993*) are chosen to demonstrate the application of the present approximate solution.

CHAPTER 2 THEORY

2.1 Unsteady 2-D chlorine transport equation

The unsteady 2-D CTE describing the concentration of total free chlorine in the water flowing through a pipe with considering first-order decay reaction is written as (*Biswas et al.*, *1993*)

$$\frac{\partial C}{\partial t}+Uf(r)\frac{\partial C}{\partial x}=D_{\mathrm{x}}\frac{\partial^2 C}{\partial x^2}+D_{\mathrm{r}}\frac{1}{r}\frac{\partial}{\partial r}\left(r\frac{\partial C}{\partial r}\right)-k_{\mathrm{d}}C \tag{1}$$

where C is the concentration of free chlorine, (mg/L); t is time, (s); U is the average flow velocity in the pipe, (m/s); r is the radial coordinate; x is the axial coordinate; D_{r} and D_{x} are the radial and axial effective diffusivities of chlorine species in the water, respectively, (m^2/s); k_{d} is the first-order decay constant in the bulk water, (1/s) and $f(r)$ is a flow parameter representing actual velocity profile as function of radial direction in a pipe and depending on the flow regime. Flow parameter, $f(r)$ is equal to $2[1-(r/r_0)^2]$ for laminar flow and is assumed approximate to 1 for turbulent flow. The first term on the left-hand side (LHS) of Eq. (1) represents the change of chlorine concentration with time in a pipe. The second LHS term represents the axial advective flux. The first and second terms on the right-hand side (RHS) of Eq. (1) account for the axial dispersive flux and the radial diffusive flux, respectively. The last RHS term is the first-order decay rate of chlorine in the bulk flow.

The associated initial and boundary conditions of Eq. (1) are as follows:

$$C(r,x,0)=C_{\mathrm{initial}}(x) \tag{2}$$

$$C(r,0,t)=C_{\mathrm{inletl}}(t) \tag{3}$$

$$C(r,\infty,t)=0 \tag{4}$$

$$\left.\frac{\partial C(r,x,t)}{\partial r}\right|_{r=0}=0 \tag{5}$$

$$D_{\mathrm{r}}\left.\frac{\partial C(r,x,t)}{\partial r}\right|_{r=r_0}=-w_{\mathrm{d}}C(r_0,x,t) \tag{6}$$

where r_0 is the pipe radius, (m); and w_d is the pipe wall surface reaction constant and also referred to "intrinsic wall decay constant", (m/s). The initial concentration $C_{initial}$ may be spatially distributed along the axial direction in a pipe and the inlet concentration C_{inlet} may vary with time. Note that the chlorine concentration is well mixed over the cross-section.

Under the turbulent condition, Eq. (1) can then be cast in the following dimensionless form as:

$$\frac{\partial C}{\partial T}+\frac{\partial C}{\partial X}=\frac{1}{P_L}\frac{\partial^2 C}{\partial X^2}+\frac{D}{R}\frac{\partial}{\partial R}\left(R\frac{\partial C}{\partial R}\right)-KC \tag{7}$$

subject to the dimensionless initial and boundary conditions

$$C(R,X,0)=C_{initial}(X) \tag{8}$$

$$C(R,0,T)=C_{inletl}(T) \tag{9}$$

$$C(R,\infty,T)=0 \tag{10}$$

$$\left.\frac{\partial C(0,X,T)}{\partial R}\right|_{R=0}=0 \tag{11}$$

$$\left.\frac{\partial C(R,X,T)}{\partial R}\right|_{R=1}=-WC(1,X,T) \tag{12}$$

where $T = tU/L$, $X = x/L$, $R = r/r_0$, $P_L = LU/D_x$, $D = LD_r/r_0^2U$, $K = k_dL/U$, and $W = w_dr_0/D_r$. The dimensionless parameters D, K, and W represent the radial effective diffusivity, the chlorine decay rate constant in the bulk water, and pipe wall surface reaction constant, respectively. If the decay reactions occurring in the bulk water and at the pipe wall are assumed the first-order kinetics, the initial concentration and inlet concentration are respectively expressed as

$$C_{initial}(X)=\hat{\beta}\exp(-\hat{\alpha}X) \tag{13}$$

and

$$C_{inlet}(T)=\tilde{\beta}\exp(-\tilde{\alpha}T) \tag{14}$$

where the $\hat{\beta}$ and $\tilde{\beta}$ are the concentration parameter (mg/L) and $\hat{\alpha}$ and $\tilde{\alpha}$ are the dimensionless reaction parameter. A diagram of control volume in a dimensionless form

for chlorine concentration in a pipe with related initial and inlet conditions is illustrated in Figure 1.

2.2 Analytical solution

Eq. (7) with the initial and boundary conditions, Eqs. (8) - (12), describes the transient chlorine transport in a pipe. The closed-form solution to Eqs. (7) - (12) can be obtained through utilization of Laplace transform with respect to time and generalized Fourier series expansion, which simplifies the differential term in the radial direction. The detailed derivation of the solution is shown in Appendix A and the Laplace-domain solution is

$$\overline{C}(R,X,s)=\sum_{n=1}^{\infty}\frac{2J_1(\lambda_n)J_0(\lambda_n R)}{\lambda_n\left[J_1^2(\lambda_n)+J_0^2(\lambda_n)\right]} \left\{\left[\frac{\tilde{\beta}}{(s+\tilde{\alpha})}+\frac{\hat{\beta}}{\left(\hat{\alpha}^2/P_L+\hat{\alpha}-\Gamma_n-s\right)}\right]\exp\left[\frac{P_L X}{2}\left(1-\sqrt{1+\frac{4}{P_L}(\Gamma_n+s)}\right)\right] -\frac{\hat{\beta}}{\left(\hat{\alpha}^2/P_L+\hat{\alpha}-\Gamma_n-s\right)}\exp(-\hat{\alpha}X)\right\} \quad (15)$$

where $\overline{C}$ is the concentration in Laplace domain; s is a Laplace parameter related to T; Γ_n is equal to $(K + \lambda_n^2 D)$; J_0 and J_1 are the zero and first order Bessel functions, respectively; and λ_n is the nth root of following equation.

$$\lambda_n J_1(\lambda_n)-WJ_0(\lambda_n)=0 \quad (16)$$

After taking Laplace inverse transform of Eq. (15), the solution for the cup-mixing average concentration C_{av} can be expressed as

$$C_{av}=\sum_{n=1}^{\infty}\Psi_n\times\left\{\tilde{\beta}\exp(-\tilde{\alpha}T)A(X,T)-\hat{\beta}\exp\left[\left(\hat{\alpha}/P_L+\hat{\alpha}-\Gamma_n\right)T\right]\left[B(X,T)-\exp(-\hat{\alpha}X)\right]\right\} \quad (17)$$

where Ψ_n is $[4W / \lambda_n^2(\lambda_n^2 + W)]$ and $A(X, T)$ and $B(X, T)$ are respectively expressed as

$$A(X,T)=\frac{1}{2}\left\{\exp\left(\frac{P_L X}{2}\left(1+\sqrt{4\eta_n/P_L}\right)\right)\times\operatorname{erfc}\left(\frac{X}{2}\sqrt{\frac{P_L}{T}}+\sqrt{\eta_n T}\right) +\exp\left(\frac{P_L X}{2}\left(1-\sqrt{4\eta_n/P_L}\right)\right)\times\operatorname{erfc}\left(\frac{X}{2}\sqrt{\frac{P_L}{T}}-\sqrt{\eta_n T}\right)\right\} \quad (18)$$

$$B(X,T)=\frac{1}{2}\left\{\exp\left(\frac{P_L X}{2}\left(1+\sqrt{4\omega/P_L}\right)\right)\times\operatorname{erfc}\left(\frac{X}{2}\sqrt{\frac{P_L}{T}}+\sqrt{\omega T}\right)\right.$$
$$\left.+\exp\left(\frac{P_L X}{2}\left(1-\sqrt{4\omega/P_L}\right)\right)\times\operatorname{erfc}\left(\frac{X}{2}\sqrt{\frac{P_L}{T}}-\sqrt{\omega T}\right)\right\} \tag{19}$$

The variable η_n in Eq. (18) and ω in Eq. (19) are defined as $(\Gamma_n-\tilde{\alpha}+P_L/4)$ and $(\hat{\alpha}^2/P_L+\hat{\alpha}+P_L/4)$, respectively. If neglecting the axial dispersion (i.e., $P_L\rightarrow\infty$), Eq. (17) can be reduced to

$$C_{av}=\sum_{n=1}^{\infty}\Psi_n\times\left\{\hat{\beta}\exp\left[\hat{\alpha}(T-X)\right]\exp(-\Gamma_n T)\times H(X-T)\right.$$
$$\left.+\tilde{\beta}\exp\left[\tilde{\alpha}(X-T)\right]\exp(-\Gamma_n X)\times H(T-X)\right\} \tag{20}$$

where the symbol H represents the Heaviside function. If inlet concentration is equal to constant, $\tilde{\beta}$ (i.e., $\tilde{\alpha}=0$), Eq. (20) under steady state can be reduced to the analytical solution developed by *Biswas et al.* (*1993*), written as

$$C_{av}=\tilde{\beta}\times\sum_{n=1}^{\infty}\Psi_n\times\exp(-\Gamma_n X) \tag{21}$$

To compute C_{av}'s using Eqs. (17), (20) and (21), the roots of the Eq. (16), λ_n, must be determined first. Eq. (16) is a nonlinear equation and its roots λ_n's can be determined by Newton's method which has the advantage of quadratic convergence in finding the roots (*Yeh*, *1987*). The C_{av} can be calculated at any location and time in the pipe if the values of λ_n's, P_L, *D, K,* and *W* are known. The C_{av}'s in Eqs. (17), (20) and (21) are represented as an infinite series; however, the relative error in estimating C_{av} is less than 5% if only the first term of the series is computed. Therefore, it may be appropriate to use the first three terms of the series in Eqs. (17), (20) and (21) to compute C_{av}.

2.3 Approximate solution

2.3.1 *Biswas et al.*'s approximate solution (*1993*)

In the case of no chlorine consumption at the pipe wall (i.e., $W = 0$) for Eq. (21), the cup-mixing average chlorine concentration can be expressed as (*Biswas et al.*, *1993*):

$$C'_{av} = \tilde{\beta} \exp\left(-KX\right) \tag{22}$$

A fractional error ε was defined to simplify the analytical solution as (*Biswas et al.*, *1993*):

$$\varepsilon = \left(C'_{av} - C_{av}\right) / C_{av} \tag{23}$$

Substituting Eq. (22) into Eq. (23), C_{av} becomes

$$C_{av} = \frac{\tilde{\beta} \exp\left(-KX\right)}{\left(1+\varepsilon\right)} \tag{24}$$

Once ε is assigned, the C_{av} can then be determined by Eq. (24). *Biswas et al.* (*1993*) used the regression technique to express ε in terms of D and W as

$$\varepsilon = 2.4416DW - 0.1559DW^2 \quad \text{for} \quad 0.01 \le W \le 10 \tag{25}$$

Eq. (24) along with Eq. (25) was then used to approximate Eq. (21) in computing the C_{av}.

2.3.2 New approximate solution

The C_{av} may be approximated by retention of the first term of the infinite series and neglect of higher order terms in Eq. (21) as

$$C_{av} = \tilde{\beta} \times \Psi_1 \times \exp\left[-\Gamma_1 X\right] \tag{26}$$

For $0 \le \lambda_n \le 12$, the Bessel functions J_0 and J_1 in Eq. (16) can be respectively written as (*Yang and Yeh*, *2002*)

$$J_0\left(\lambda_n\right) = 1 - \frac{\frac{1}{4}\lambda_n^{\,2}}{(1!)^2} + \frac{\left(\frac{1}{4}\lambda_n^{\,2}\right)^2}{(2!)^2} - \frac{\left(\frac{1}{4}\lambda_n^{\,2}\right)^3}{(3!)^2} + \cdots \tag{27}$$

and

$$J_1\left(\lambda_n\right) = \left(\frac{\lambda_n}{2}\right)\left[1 - \frac{\frac{1}{4}\lambda_n^{\,2}}{(1!)(2!)} + \frac{\left(\frac{1}{4}\lambda_n^{\,2}\right)^2}{(2!)(3!)} - \frac{\left(\frac{1}{4}\lambda_n^{\,2}\right)^3}{(3!)(4!)} + \cdots\right] \tag{28}$$

The value of λ_n increases with W which equals $w_d r_0/D_r$. D_r, is assumed to equal to the eddy diffusivity suggested by *Edwards et al.* (*1979*) as $D_{eddy} = 1.233\times10^{-2}Ur_0$. *Rossman et al.* (*1994*) used EPANET program to simulate chlorine residual in the network in New Haven, Connecticut including 41 pipes and 36 nodes where the range for the value of W is form 7.3×10^{-4} to 7.0×10^{-2} under turbulent flow. This network was also studied by *Biswas et al.* (*1993*) and W ranges from 1.49×10^{-5} to 1.3×10^{-2}. Additionally, in the experimental study for chlorine decay, the value of W is about from 2.49×10^{-4} to 3.48×10^{-3} under turbulent flow (e.g., *Ozdimer and Ger*, *1998*; *Rossman et al.*, *2001*; *Rossman*, *2006*). The value of W is considered smaller than 0.1. The first root λ_1 is less than 0.5 when $W < 0.1$. Therefore, the third and higher order terms in Eq. (27) and the second and higher order terms in Eq. (28) are relatively small and negligible. Accordingly, based on Eq. (16), λ_1 becomes

$$\lambda_1 = \sqrt{\frac{4W}{2+W}} \tag{29}$$

Eq. (26) can then be expressed as

$$C_{av} = \tilde{\beta}\times\left(1+\frac{2W}{4+2W+W^2}\right)\exp\left[-\left(K+\frac{4DW}{2+W}\right)X\right] \tag{30}$$

As an approximate solution to Eq. (21), Eq. (30) is very simple and easy to use to compute the C_{av}. When W is smaller than 0.1, the second term on the RHS of Eq. (30) is much less than 1. Thus, the approximate solution is further simplified to

$$C_{av} = \tilde{\beta}\exp\left[-\left(K+\frac{4DW}{2+W}\right)X\right] \tag{31}$$

CHAPTER 3 METHODOLOGY OF PRESENT MODEL

3.1 Hydraulic time step and water quality time step

Before simulating the chlorine residual in a water distribution system by a water quality model, the hydraulic simulation should be performed first. The water-use rate at every node in a water distribution system is taken as an average value within a discrete time interval, t_h, called the hydraulic time step (HTS). The computer program such as EPANET (*Rossman et al.*, *1994*) or KYPIPEF (*Wood*, *1986*) can be used with known pipe information and nodal water-use rates to perform hydraulic simulation for all the necessary HTSs. The average flow velocities in pipes for all the HTSs can then be obtained from the hydraulic simulations. A HTS is usually divided into several water quality time steps (WQTSs), t_s. *Rossman et al.* (*1994*) used a time interval of 1 hr in their hydraulic simulation and a smaller time step dependent on the pipe length and flow velocity for simulating chlorine transport in the water networks. Thus we also use 1 hr for the HTS when performing the hydraulic simulation and a smaller time interval such as 1 min for the WQTS.

3.2 Segment of a pipe

For simulating the chlorine transport in a water network, the influence of axial dispersion on the chlorine transport is small and, therefore, negligible in comparison with the axial advection. In addition, the fluid velocity is considered uniform over the pipe cross-section; in other words, the water network has plug flow in pipes. At the beginning of the first HTS, each pipe is considered as a segment and the concentration in each pipe (i.e., initial concentration) is assumed as uniform (well-mixed) and equal to the observed concentration at its downstream node. Figure 2 shows an example of the chlorine transport, which acts as plug flow, in a single pipe line at the first HTS, i.e., from $t = 0$ to $t = t_h$, for the flow from left to right. The black, gray, and light gray colors denote the water residing in the pipes j+1, j, and j-1, respectively, at the beginning of simulation. At $t = t_h/3$, pipe j may contain gray and

light gray water because a part of water in pipe j-1 (in light gray color) flows into pipe j. At $t = 2t_h/3$, the water originally resides in pipe j-1 at $t = 0$ may all flow into the pipe j if the hydraulic retention time of water in pipe j-1 is equal to $2t_h/3$. At the end of the first HTS (i.e., $t = t_h$), a part of the water originally resides in pipe j may still stay in pipe j. We refer to this portion of pipe as segment 1 for the second HTS and marked with grey color which is the last panel in Figure 2. This panel also demonstrates that the water originally resides in pipe j-1 and now all stays in the segment 2 of pipe j for the second HTS. Moreover, the third segment for the second HTS (with white color) in pipe j is occupied by the water originally residing in pipe j-2. Therefore, in the second and succeeding HTSs, each pipe is divided into a number of segments dependent upon the pipe length, flow velocity, and the origin at previous HTS for water residing in each pipe at beginning of HTS. Therefore, the water within a segment of a pipe at beginning of HTS comes from the same segment at the previous HTS or treatment plant. Different pipes may have different diameter and thus are of different hydraulic radius and radial effective diffusivity. Therefore, at beginning of each HTS, the number of segments in each pipe should be determined in order to predict the spatial distribution of chlorine concentration in the pipe network at every HTS using the present analytical solution. In addition, the number of segments in a pipe is in an order starting from the outlet node and ending at the inlet node.

3.3 Flow time for water in different segments

The dimensionless axial location in pipe j is denoted as X_j and the retention time in pipe j is PT_j^m. The retention times of ith and vth segments of pipe j at the mth HTS are denoted as $ST_{i,j}^m$ and $ST_{v,j}^m$, respectively. In pipe j, when water at the end of the vth segment flows to X_j at mth HTS, the arrival time is equal to $\sum_{i=1}^{v-1} ST_{i,j}^m - PT_j^m\left(1-X_j\right)$ in which the first term is the retention time for water at the end of the segment to the end of pipe j and the second is the retention time for water flow from X_j to the end of pipe j. Therefore, at mth HTS, the flow

time for water in the vth segment of pipe j passing through X_j ranges from $\sum_{i=1}^{v-1} ST_{i,j}^m - PT_j^m\left(1-X_j\right)$ to $\sum_{i=1}^{v} ST_{i,j}^m - PT_j^m\left(1-X_j\right)$. Moreover, the arrival time for water in the vth segment of upstream pipe k when passing through X_j at mth HTS can be divided into three time intervals. The first interval is $\sum_{i=1}^{v-1} ST_{i,k}^m$ representing the retention time for water at the end of the vth segment to the outlet node of pipe k; the second is $\sum_{i=k+1}^{j-1} PT_i$ standing for the retention time for water at the outlet node of pipe k to the inlet node of pipe j and the last is $PT_j \times X_j$ denoting the retention time for water at the inlet node of pipe j to X_j. Thus, the flow time for water in the vth segment of upstream pipe k passing through X_j starts from $\sum_{i=1}^{v-1} ST_{i,k}^m + \sum_{i=k+1}^{j-1} PT_i + PT_j \times X_j$ and ends at $\sum_{i=1}^{v} ST_{i,k}^m + \sum_{i=k+1}^{j-1} PT_i + PT_j \times X_j$.

3.4 Concentration distribution in a pipe line predicted by the present model

Based on Eq. (13), the initial spatial distribution of chlorine concentration in the vth segment of pipe j at the mth HTS can be expressed as

$$C_{\text{initial}\,v,j}^{\ m} = \hat{\beta}_{v,j}^m \exp\left(-\hat{\alpha}_{v,j}^m X_j\right) \tag{32}$$

where $\hat{\beta}_{v,j}^m$ and $\hat{\alpha}_{v,j}^m$ respectively denote the concentration and dimensionless reaction parameters in the vth segment of pipe j at the mth HTS.

Eq. (20) which is expressed in terms of an infinite series can be used to describe the cup-mixing average concentration, C_{av}. For the ease of computing, this term is used to develop the analytical model for the simulation of chlorine concentration distribution in a single pipe. Accordingly, the concentration at X_j within pipe j at mth HTS is

$$C_{av\,j}^{\ m} = \psi_j^m \times \hat{\beta}_{v,j}^m \exp\left[\hat{\alpha}_{v,j}^m\left(T_j^m - X_j\right)\right]\exp\left[(-\gamma_j^m)T_j^m\right] \quad \text{for} \quad \sum_{i=1}^{v-1} ST_{j,i}^m - PT_j^m\left(1-X_j\right) < \tau < \sum_{i=1}^{v} ST_{j,i}^m - PT_j^m\left(1-X_j\right) \tag{33}$$

where τ is the time within a HTS raging from 0 to t_h, T_j^m is a dimensionless time of pipe j and equal to τ divided by the retention time of pipe j, and γ_j^m and ψ_j^m represent Ψ_1 and Γ_1 for the pipe j at the mth HTS, respectively. Based on Eq. (33), the concentration distribution at the outlet node in pipe j (i.e., $X_j = 1$) can be written as

$$C_{avj}^{m} = \psi_j^m \times \hat{\beta}_{v,j}^m \exp\left(-\hat{\alpha}_{v,j}^m\right)\exp\left[-(\gamma_j^m + \hat{\alpha}_{v,j}^m)T_j^m\right] \qquad \text{for} \quad \sum_{i=1}^{v-1} ST_{i,j}^m < \tau < \sum_{i=1}^{v} ST_{i,j}^m \tag{34}$$

This equation can also be used to describe the concentration distribution at the inlet node of pipe j+1 if the T_j^m in Eq. (34) is changed to T_{j+1}^m because the retention times for water flow in pipes j and j+1 may be different. The relationship between the variables T_j^m and T_{j+1}^m can be expressed by mean of the parameter $\theta_{j+1,j}^m$, which is the ratio of PT_{j+1}^m to PT_j^m, so the variable T_j^m is equal to $\theta_{j+1,j}^m$ multiplied by T_{j+1}^m. Based on the second term on the RHS of Eq. (20), the concentration distribution at X_{j+1} for water coming from the vth segment of pipe j can be obtained by the relationships of $\tilde{\beta} = \psi_j^m \hat{\beta}_{v,j}^m \exp\left(-\hat{\alpha}_{v,j}^m\right)$ and $\tilde{\alpha} = \theta_{j+1,j}^m(\hat{\alpha}_{v,j}^m - \gamma_j^m)$.

Similarly, the concentration distribution at X_j for water coming from the vth segment of the upstream pipe k can be written as

$$C_{avj}^{m} = \prod_{i=k}^{j} \psi_i^m \times \hat{\beta}_{v,k}^m \exp\left[-\left(\hat{\alpha}_{v,k}^m + \sum_{i=k+1}^{j-1}\gamma_i^m + (\hat{\alpha}_{v,k}^m - \gamma_k^m)\sum_{i=k+1}^{j-1}\theta_{i,k}^m\right)\right] \times \exp\left[\theta_{j,k}^m(\hat{\alpha}_{v,k}^m - \gamma_k^m)\left(T_j^m - X_j\right)\right]\exp\left(-\gamma_j^m X_j\right) \tag{35}$$

$$\text{for} \quad \sum_{i=k+1}^{j-1} PT_i + \sum_{i=1}^{v-1} ST_{i,k}^m + PT_j \times X_j < \tau < \sum_{i=k+1}^{j-1} PT_i + \sum_{i=1}^{v} ST_{v,k}^m + PT_j \times X_j$$

The concentration distribution at any location in a pipe line can be estimated at every WQTS using Eq. (33) for $k = j$ or Eq. (35) for $k \neq j$ once the retention time in every segment within

the HTS and the upstream segment, which the passing water at the location X_j within the WQTS comes from, are determined.

3.5 Searching the segment within a water quality time step

At the mth HTS, the flow time is $\sum_{i=k+1}^{j} PT_i^m - (1-X_j)PT_j^m$ for water at the end of pipe k ($k \leqq j$) to arrive at X_j. Similarly, the flow time is $\sum_{i=k+1}^{j} PT_i^m - (1-X_j)PT_j^m + \sum_{i=1}^{v-1} ST_{i,k}^m$ for water at the end of the segment v in pipe k to arrive at X_j. Therefore, the segment in which the water passes through X_j at time τ can be determined based on the following relationship:

$$\sum_{i=1}^{v-1} ST_{i,k}^m < \tau - \left[\sum_{i=k+1}^{j} PT_i^m - (1-X_j)PT_j^m \right] < \sum_{i=1}^{v} ST_{i,k}^m \tag{36}$$

3.6 Segment division in a pipe line at each hydraulic time step

At the first HTS, the length of segment in each pipe is equal to the pipe length; thus, the retention time of each segment equals the pipe length divided by the average flow velocity. The dimensionless time at the end of the mth HTS in pipe j, $T_j'^m$, is equal to t_h / PT_j^m. Consider that the water passing through the outlet node of pipe j at the end of mth HTS comes from v'th segment of pipe k'. The variables k' and v' can be determined by Eq. (36) when $X_j = 1$ and $\tau = t_h$. However, the water in v'th segment of pipe k' may not reside completely in pipe j at the end of mth HTS because a part of the water may travel through the outlet node of pipe j. The flow time for the water in v'th segment of pipe k' passing through the outlet node of pipe j is equal to $(t_h - \sum_{i=k'+1}^{j} PT_i^m - \sum_{i=1}^{v'-1} ST_{i,k}^m)$. The remaining part of the water staying in pipe j becomes the first segment of pipe j at the (m+1)th HTS and its flow time is $[ST_{k',v'}^m - (t_h - \sum_{i=k'+1}^{j} PT_i^m - \sum_{i=1}^{v'-1} ST_{i,k}^m)]$. Therefore, the retention time for the first segment of pipe j at the (m+1)th HTS, $ST_{1,j}^{m+1}$ is $u_j^m[ST_{k',v'}^m - (t_h - \sum_{i=k'+1}^{j} PT_i^m - \sum_{i=1}^{v'-1} ST_{i,k}^m)]/u_j^{m+1}$ where

u_j^m and u_j^{m+1} are the average flow velocities in pipe j at the mth and (m+1)th HTS, respectively.

The water in the second segment of pipe j at the (m+1)th HTS may come from a whole segment situated at the upstream of the v'th segment in pipe k'. Therefore, the retention time for water in the 2nd segment $ST_{2,j}^{m+1}$ is equal to $u_j^m(ST_{1,k-1}^m)/u_j^{m+1}$ if the v'th segment is the last segment in pipe k' or $u_j^m/u_j^{m+1}(ST_{v'-1,k}^m)$ if the v'th segment is not the last one. Similarly, the retention times for succeeding segments in pipe j at the (m+1)th HTS except for the last one can then be determined.

The sum of the retention time for water in each segment within a pipe must equal the hydraulic retention time for water flowing through the pipe j. If the sum of the retention time for water from the first segment to the Nth segment is greater than or equal to the hydraulic retention time of pipe j, the Nth segment is indeed the last segment of pipe j. Thus, the retention time for water in the Nth segment $ST_{N,j}^{m+1}$ is equal to $PT_j^{m+1} - \sum_{i=1}^{N-1} ST_{i,j}^{m+1}$.

The initial concentration distribution in each segment at the (m+1)th HTS can be determined based on Eq. (33) or (35), once the origin of the water in each segment of pipe j at the (m+1)th HTS is known. For example, the concentration distribution in the first segment at the (m+1)th HTS can be determined with known $T_j'^m$, v', and k' according to Eq. (33) if $k' = j$ or Eq. (35) if $k' \neq j$.

3.7 Network

In a water network, there may be more than one pipe connected to a node. Assume that the concentration at the confluent node is well mixed and its concentration, C_m, can be calculated as (*Rossman et al., 1994*)

$$C_{\mathrm{m}} = \sum_{I \in G} \left(\frac{\prod_{i \in g} q_{\mathrm{i}}}{\prod_{i \in g} Q_{\mathrm{i}}} C_{\mathrm{av\,j}}^{\ \mathrm{m}} \right)_I \tag{37}$$

where G is the number of flow path, g is the number of confluent node in a flow path, Q_{i} is the total flow rate at confluent node i, and q_{i} is the flow rate at confluent node i in a single flow path. Figure 3 shows an example network which comprises nine pipes, seven nodes, and two confluent nodes denoted as black circles. For the outlet node in pipe 9, there are three flow paths. Path 1 includes pipes 1, 2, 3, 5, 6 and 9; path 2 has pipes 1, 2, 4, 6, and 9; path 3 contains pipes 1 and 7 to 9. Based on Eq. (37), the mixing concentration at the outlet node of pipe 9 is

$$C_{\mathrm{m}} = \frac{q_5 \times q_6}{(q_4 + q_5)(q_6 + q_8)} \left(C_{\mathrm{av9}}^{\ \mathrm{m}} \right)_1 + \frac{q_4 \times q_6}{(q_4 + q_5)(q_6 + q_8)} \left(C_{\mathrm{av9}}^{\ \mathrm{m}} \right)_2 + \frac{q_6}{(q_6 + q_8)} \left(C_{\mathrm{av9}}^{\ \mathrm{m}} \right)_3 \tag{38}$$

3.8 Flowchart of water quality simulation

The flowchart for the simulation of chlorine concentration in a water network using the present model is illustrated in Figure 4. The flowchart includes three parts. The first part is to set the initial condition of the retention time and the initial concentration distribution in each segment for each flow path at the fist HTS. Then, the present model is proceeding to the second part for the estimation of the chlorine concentration at each WQTS. The second part, which includes the main solution algorithm of the present model, includes three steps. The first step is to determine the vth segment of pipe k for each flow path in which the water passes through the location X_{j} at the current WQTS using Eq. (36). The second step is to calculate the chlorine concentration in each flow path using Eq. (33) or (35) and the last step is to calculate the mixed concentration for the current WQTS by Eq. (37). The last part is to determine the retention times and concentration distribution in each segment for all flow paths for the next HTS. Then, the algorithm of the present model will go back to the second part to estimate the chlorine concentration for the next HTS. When accomplishing all the HTSs, the analytical model will complete the network concentration simulations.

CHAPTER 4 RESULTS AND DISCUSSION

4.1 Accuracy comparisons of the approximate solutions

The present approximate solution is compared with both the analytical and approximate solutions given in *Biswas et al.* (*1993*). Three figures are plotted to investigate the effect of the parameters D, K, and W on the corresponding predicted chlorine concentration. Figures 5(a), 5(b) and 5(c) show the curves for the chlorine concentration distribution of, C_{av} with initial concentration equal to one, at the outlet ($X = 1$) versus the dimensionless wall decay rate (W) with different values of dimensionless radial diffusivity (D) for the dimensionless water decay rate (K) equal to 0.001, 0.1 and 1. The solid line, dotted line, and dashed line represent the analytical solution, present approximate solution, and *Biswas et al.*'s approximate solution (*1993*), respectively.

As indicated in Figures 5(a) - (c) for different K values, the value of C_{av} based on *Biswas et al.*'s approximate solution (*1993*), starts to be different from the analytical solution for W at 0.003, 0.03 and 0.3 when D = 100, 10, and 1, respectively. The present approximate solution is in good agreement with the analytical solution for K ranging from 0.001 to 1 with D equals 100, 10, and 1 except in the region where $W > 0.5$ and $K = 1$. Those results indicate that the parameters of D and W have an apparent influence on the accuracy of those two approximate solutions. In addition, the present approximate solution generally gives better prediction for the chlorine concentration than that of *Biswas et al.*'s approximate solution (*1993*).

The poor accuracy of the *Biswas et al.*'s approximate solution (*1993*) stems from the fact that the expressions of fractional factor, ε, in terms of D and W were developed using the regression techniques as shown in Eq. (25). On the other hand, the error of the present approximate solution is made mainly by neglecting the higher order terms of the Bessel

functions in Eqs. (27) and (28). If the first eigenvalue λ_1 is small, the errors of neglecting the high order terms in the Bessel functions of Eqs. (27) and (28) will be very small.

Figure 6 shows the plots of the true and approximate values of λ_1 against W. The solid line represents the true λ_1 obtained from Eq. (16) by Newton's method and the dashed line denotes the approximate λ_1 calculated from Eq. (29). This figure indicates that both the value of λ_1 and the difference in λ_1 increase with W. In addition, Table 1 shows the relative errors of the approximate λ_1 to the true λ_1 for W ranging from 0.001 to 0.5 and the relative error is about 1.2 % at $W = 0.1$. Accordingly, the present approximate solution gives accurate results when $W < 0.1$ and is thus appropriate for most of field cases.

4.2 Two case studies for the approximate solution

The first-order reaction kinetics is usually used to represent the chlorine decay in the bulk liquid of the pipe and at the pipe wall. The decay parameters can be determined based on an appropriate mathematical model and measured chlorine concentration data. Two cases are chosen to demonstrate the application of the present approximate solution. The wall surface reaction constant estimated based on the approximate solution is compared with those obtained from *Biswas et al.* (*1993*) and *Rossman* (*2006*) in Case 1 and from the water network of SCCRWA (*Biswas et al.*, *1993*) in Case 2.

4.2.1 Case 1

Rossman (*2006*) used a distribution system simulator which consisted of a 27 m long loop with 0.15 m diameter unlined ductile iron pipe, a recirculation pump and a heat exchanger cooling system. An experiment was made to measure the reaction rate of chlorine in a simulated pipe for water treated by different forms of advanced treatment at US EPA's Test and Evaluation Facility in Cincinnati, Ohio. In Case 1, the present approximate solution is used to determine the pipe wall surface reaction constants w_d for water applied by three different treatments. The initial chlorine was about 6 mg/L and the values of k_d shown in the second column of Table 2 (*Rossman*, *2006*) for lab-tested water under different

treatments were determined based on the analysis of the kinetic test data. The wall surface reaction constants, w_d, for three sorts of lab-tested water can then be determined from the experiment-observed data based on the present approximate solution. In the experiment, the flow velocity was maintained constant, so steady-state flow condition was considered. Note that the axial distance from the inlet along the pipe, x, is equal to the flow velocity multiplied by the flow time in pipe. Under the turbulent condition, the eddy diffusion is greater than the molecular diffusion. Thus, the effective diffusivity in the radial direction, D_r, is only considered the eddy diffusivity which can be obtained from *Edwards et al.* (*1979*) because of turbulent flow. With the known values of pipe radius, pipe length, flow velocity, and chlorine bulk decay constant, w_d can be determined based on the present approximate solution, Eq. (31), when minimizing the objective function defined as the sum of square errors between the observed and predicted chlorine concentrations. In order to determine the optimal value of w_d for three sorts of lab-tested water, simulated annealing (SA) is applied. The SA is a generic probabilistic meta-algorithm for the global optimization problem based on the annealing concept, namely locating a good approximation to the global optimum of an objective function in a large search space. The initial temperature of the SA is chosen as 100 and the temperature is decreased by the temperature reduction factor (0.85) after 8100 calculations. The annealing process will be terminated if the absolute differences between two successive objective function values are all less than 10^{-10} within 20 iterations or the number of evaluations is greater than 10^7. The SA has been successfully applied in forecasting THM Species (*Lin and Yeh*, *2005*), parameter estimations (e.g., *Yeh and Chen*, *2007*; *Yeh et al.*, *2007a*), and source identifications (e.g., *Lin and Yeh*, *2007*; *Yeh et al.*, *2007b*).

As suggested by *Rossman* (*2006*), a first-order reaction model for describing the first-order decay of chlorine in bulk flow and at the pipe wall was expressed as

$$\frac{\partial C}{\partial t} = -\left(k_{\mathrm{d}} + \frac{w_{\mathrm{d}}}{r_{\mathrm{h}}} \right) C \tag{39}$$

where r_{h} is hydraulic radius of pipe. Table 2 lists the w_{d} estimated by the present approximate solution, the first-order reaction model (*Rossman*, *2006*), and *Biswas et al.*'s approximate solution (*1993*) for three sorts of lab-tested water. The table shows that the values of w_{d} estimated by these three models are close for the same lab-tested water. Note that the first-order reaction model neglects the radial diffusion and thus the estimated w_{d} slightly differs from those given by the other two solutions. Figure 7 shows the experiment-observed data (*Rossman*, *2006*) and the simulated results by the present approximate solution and *Biswas et al.*'s approximate solution (*1993*). The solid line represents the result of the present approximate solution and the dashed line represents the result of *Biswas et al.*'s approximate solution (*1993*). The symbols of circle, rhombus, and triangle displayed in Figure 7 denote experiment-observed values for lab-tested water treated by reverse osmosis, conventional treatment, and ozonation, respectively. This figure indicates the simulated results of the present approximate solution are in good agreement with experiment-observed values from *Rossman* (*2006*). In contrast, the simulated results of *Biswas et al.*'s approximate solution (*1993*) are discordant in the case of the lab-tested water treated by ozonation with greater w_{d} value. This problem may be attributed to the fact that the chlorine concentration is inversely proportional to the quadratic of wall decay constant in *Biswas et al.*'s approximate solution (*1993*) as expressed in Eqs. (24) and (25). Chlorine concentration is considered to decay exponentially with increasing retention time as indicted in Eq. (39) and thus the chlorine concentration is inversely proportional to the exponent of k_{d} and w_{d}. The present approximate solution expressed as Eq. (31) conforms to the form of the first-order decay reaction. This may be the reason why the simulated results of the present approximate solution are better than those of *Biswas et al.*'s approximate solution (*1993*) when w_{d} is large.

4.2.2 Case 2

In Case 2, the present approximate solution is employed to determine the w_d in a field test conducted by the SCCRWA in New Haven, Connecticut. The service area of this network covers 5.2 km^2 and the network is composed of a storage tank, a pump station, 40 pipes ranging from 76 to 731 m with constant diameters of 20.3 and 30.5 cm, and totally 36 nodes. The schematic of this network is shown in Figure 8 which includes eight sample points denoted by the words "SP". The sampling results of chlorine concentration at the inlet and outlet points of these pipe segments are presented in the second and third columns of Table 3 (*Biswas et al.*, *1993*). The geometrical and flow parameter including pipe length, pipe radius, flow velocity (*Biswas et al.*, *1993*) and diffusion coefficients for all the pipes are listed in Table 4. The diffusion coefficients were determined by the eddy diffusivity, as obtained from *Edwards et al.* (*1979*). In addition, the chlorine bulk decay constant, k_d, was 6.4×10^{-6} (1/s) (*Biswas et al.*, *1993*) obtained by bench kinetic tests performed with the water sample taken at the inlet to the network.

In pipes 1 to 3, 6 to 16, 21, and 26 to 28 of this network (Figure 8), those pipes numbered 3, 10 and 21 are dead end pipes while the other pipes are main branch. The present approximate solution expressed in Eq. (31) is used to determine the wall surface reaction constant, w_d, in this network. The average value of w_d for the main pipes such as 7, 9, 11 to 15, and 26 to 28 in this network can be determined first. Assume that the wall surface reaction constant for the main pipes are all the same because those pipes were made by the same material. Based on Eq. (31), the average concentrations at $X = 1$, the outlet of pipe 7, can be expressed as

$$C_{\text{av}\,7} = C_{\text{in}\,7} \times \exp\left[-\left(K_7 + \frac{4D_7W_7}{2+W_7}\right)\right] \tag{40}$$

The subscript in each variable represents the pipe number and $C_{\text{in}\,7}$ is the inlet concentration of pipe 7. The average concentrations at the outlet of other main pipes can be expressed in a

similar manner. The chlorine concentrations are only measured at the inlet and outlet nodes of the segment and a segment usually contains several pipes. The outlet concentration of a pipe is in fact the inlet concentration of the next pipe. Thus, the concentration C_{av} at the outlet of a segment is equal to the product of C_{av} of each pipe within the segment. The concentration at the outlet of pipe 28, $C_{out\,28}$ in the segment containing main pipes 7, 9, 11 to 15 and 26 to 28 can be written as

$$C_{in\,7} \times \prod_{i \in \text{main pipes}} \exp\left[-\left(K_i + \frac{4D_iW_i}{2+W_i}\right)\right] = C_{out\,28} \tag{41}$$

Furthermore, Eq. (41) can be simplified and expressed in term of W as

$$\sum_{i \in \text{main pipes}} \frac{4D_iW_i}{2+W_i} = -\left[\ln(C_{out\,28}/C_{in\,7}) + \sum_{i \in \text{main pipes}} K_i\right] \tag{42}$$

where D and K are known dimensionless parameters and W is a function of w_d. Note that W equals $w_d D_r/r_0$ and is the only unknown in Eq. (42). Solving Eq. (42) by Newton's method, the average value of w_d for the main branches including pipes 7, 9, 11 to 15 and 26 to 28 is obtained as 3.47×10^{-7} (m/s). This value presents the average wall surface reaction constant in the main branch. The same approach and the main branch w_d are then employed to further evaluate the w_d for the dead ends pipes 3, 10, and 21 as shown in Figure 8. The estimated w_d including those three pipes are in the range from 3.47×10^{-7} to 1.01×10^{-5} (m/s) and listed in the last column of Table 4. Note that the value of w_d ranges from 0 to 7.06×10^{-5} (m/s) reported from field or experimental studies (*Biswas et al.*, *1993*; *Rossman et al.*, *1994*; *Vasconcelos et al.*, *1997*; *Ozdemir and Ger*, *1998*; *Munavalli and Kumar*, *2006*; *Rossman*, *2006*). With the known geometrical and flow parameters and the estimated values of w_d, the concentration C_{av} for all the segments in this network predicted by *Biswas et al.*'s analytical solution (*1993*), Eq. (21) are listed in the fifth column of Table 3.

The sampled concentrations in the inlet and outlet of segments in the network are listed in the second and third columns of Table 3, respectively. In addition, the dimensionless

sampled concentration at each segment is listed in the fourth column. The segments of pipes 7, 9, 11 and 12 to 15, 26 to 28 consist of the main branch. Table 3 lists the C_{av}/C_{in} predicted based on the analytical solution and the sampling concentration given in *Biswas et al*. (*1993*) at some inlets and outlets of the pipe segments. Table 3 indicates that the predicted C_{av}/C_{in} for the segments containing dead-end pipe agrees with the dimensionless sampling concentration (C_{out}/C_{in}) for the same segment. This demonstrates that the present approximate solution can be applied to determine w_d for the field application problem. Table 4 indicates that the w_d's in the dead-end pipes 3, 10, and 21 are much greater than those in the main branch pipes. High value of w_d denotes that wall decay is significant. *Biswas et al*. (*1993*) also mentioned that significant biofilm growth occurs in the dead-end pipe where the flow velocity is relatively low if compared with that in main branch pipe. Low water flow velocity causes more retention time in the pipe, and consequently, yields lower chlorine concentration due to the decay reaction. Once the chlorine concentration is lowered, the microorganisms formed as biofilm on the pipe wall is then increased. Consequently, the high values of pipe wall surface reaction may result in large values of w_d for the dead-end pipes 3, 10, and 21 as demonstrated in the last column of Table 4.

4.3 Network simulation

The present model is used to simulate the chlorine distribution in the water distribution system of the SCCRWA as indicated in Figure 8. The water supply network of the SCCRWA was employed as a study site many times in the past to test various water quality models (e.g., *Clark et al.*, *1993*, *1994*; *Rossman et al*., *1994*). The water flows into the network from the pump station (denoted as node 1) after the water level in the storage tank is lower than the lowest standard of water level. When the storage tank is filled, the water supply from pump station is stopped and then the water is supplied from the storage tank (denoted as node 26). The hydraulic simulation is performed using EAPNET program to determine the flow rate and velocity for all pipes in this network within 1 hr time interval over

53 sampling period with the pipe and nodal demand data given by *Rossman* (personal communication). For water quality simulation, each nodal data for the sampling chlorine concentration provided by *Rossman* (personal communication) is used as the initial concentration of the present model for its upstream pipe.

A value of 6.4×10^{-6} from the bottle test (*Rossman et al.*, *1994*) is assigned as the first-order reaction constant k_d for chlorine in the network. The flow velocities are high in pipes 1 to 7, 9 to 15 and 26 to 28 and their variations are very small within the first three HTSs. Therefore, the flow is considered steady in those pipes within the first three HTSs. There are two flows into node 25 at time equal to 3 hr. One is the treated water from pump station, which has flowed through the node 25; the other is from node 4 to node 25 at the end of third HTS, as shown in Figure 8. Note that the flow rate and chorine concentration in pipe 17, i.e., from node 17 to node 15, are very small and negligible. Initial observed concentrations at node 4 is 1.15 mg/L; the chorine concentration at the pump station is kept as a constant 1.15 mg/L and the sampling concentration at node 25 is 0.98 mg/L at the time of 3 hr. Thus, the wall reaction parameter w_d is 1×10^{-6} m/s determined by the methodology of the present approximate solution. With this w_d value, the temporal chlorine concentration distribution at the storage tank, i.e., node 26, is simulated over 53 hr using the EPANET program.

Rossman et al. (*1994*) mentioned that the determined water usages at nodes 10, 28 and 34 are not accurate; therefore, these three nodes are excluded in the simulations for the nodal chlorine concentrations. The simulated results obtained from the present model are compared with those obtained from *Rossman et al.*'s model (*1994*) computed by EPANET program and the observed data. Figures 9(a) - 9(e) show the chlorine concentration versus time at nodes 3, 6, 11, 19 and 25, respectively. The solid line represents the simulated results of the present model with the WQTS of one minute, dashed line represents the results of *Rossman et al.*'s model (*1994*) with the wall decay constant of 1.74×10^{-6} (m/s) obtained

from regression technique with all observations (*Rossman et al*., *1994*), and the dot represents the observed data. Both models, the present model and *Rossman et al.*'s model (*1994*), give good agreement with the observed data except that at node 19. As indicated in these figures, the concentration varies periodically with time due to the cyclic operation of pump station. The predicted chlorine concentrations at node 19 obtained from these two models give poor fit to the observed data. There seems a fixed time lag of several hours between the observed data and both predicted results. The existence of time lag may be attributed to the discrepancy indicated in the result of fluoride simulation shown in *Rossman et al.* (*1994*, Figure 6a).

4.4 Model comparison

The chlorine concentrations determined by the present model and *Rossman et al.*'s model (*1994*) at node 3 have obvious differences as indicated in Figure 9(a). The wall decay parameter w_d used in the present model is smaller than that used in the *Rossman et al.*'s model (*1994*). The simulated concentration at node 3 by the present model is also smaller than that of *Rossman et al.*'s model (*1994*) in the period of water supply from the storage tank. In this period, the water flow velocity in pipe 3 from node 2 to node 3 ranges from 0.006 to 0.03 (m/s) which are about one order of magnitude lower if compared with most of the flow velocities in the network. Two major differences between these two models are the dimension of the model and the mechanism for mass transfer from the bulk flow to the pipe wall. The present model is developed based on an analytical solution of 2-D CTE which utilizes the diffusive mechanism to express the chlorine transport at the pipe wall represented by Eq. (6). On the other hand, *Rossman et al.*'s model (*1994*) used a mass transfer coefficient k_f depending on Reynolds number to reflect the mass transport from the bulk flow to the pipe wall. The mass transfer coefficients under turbulent and laminar flow conditions are estimated by separate empirical equations given by *Rossman* (*2000*).

The overall decay constant is represented by $[k_d + 2w_d k_f/r_0(w_d + k_f)]$ in *Rossman et al.* (*1994*) and by $(k_d + \lambda_1^2 D_r/r_0^2)$ which has the dimensionless form of Γ_1 $(K + \lambda_1^2 D)$ in the first term of Eq. (20) in the present model. Figure 10 shows the curves for the overall decay constant versus the Reynolds number *Re* with different values of pipe radiuses when w_d equals 1×10^{-6} m/s for pipe 3 with the length of 400 m. The solid line and dashed line represent the present study and the *Rossman et al.*'s model (*1994*), respectively. In fact, the effect of the reaction constant in the bulk water on the overall decay constant is not considered in both two models.

These two overall decay constants decreases tardily in turbulent flow regime (*Re* > 2300) as indicated in Figure 10. Under laminar flow condition, the curve of the *Rossman et al.*'s model (*1994*) drops suddenly, while the curve of present model starts to decline obviously at *Re* close to 100. The mass transfer coefficient k_f under laminar flow condition is much smaller than that under turbulent flow condition based on the empirical equations given by *Rossman* (*2000*). Thus, for *Rossman et al.*'s model (*1994*), the mass transfer flux from bulk flow to the pipe wall will obviously decline and result in low overall decay constant under laminar flow condition. On the other hand, the overall decay constant in the present model has a higher value under the laminar flow condition because the diffusivity is estimated using *Edwards et al.*'s formula. (*1979*). Thus, the difference in the simulated concentrations determined by the present model and *Rossman et al.*'s model (*1994*) at node 3 is mainly caused by the presence of laminar flow.

CHAPTER 5 CONCLUSIONS

The analytical solutions for unsteady 2-D CTE in a single pipe under turbulent flow condition with and without considering axial dispersion were derived using Laplace transform and generalized Fourier series expand technique. The analytical model was then developed based on the assumption of negligible axial dispersion. This model can be used to simulate the chlorine concentration distribution in a water distribution network when using the results of hydraulic simulations given by EPANET (*Rossman et al.*, *1994*). This study also developed a new approximate solution for describing the average chlorine concentration in the pipe by mainly neglecting the high order terms in the analytical solution (*Biswas et al.*, *1993*) and Bessel functions. Generally, this approximate solution provides a better prediction for a wide range of the parameters except that the dimensionless wall decay rate is greater than 0.1. The present approximate solution has been shown to have merits of easy evaluation and good accuracy if compared with *Biswas et al.*'s approximate solution (*1993*).

The approximate solution can be used either to predict the chlorine decay in pipes or to determine the wall decay parameter if coupled with an optimization algorithm such as the simulated annealing. Two cases were chosen to demonstrate the application of the present approximate solution. In the first case, the approximate solution coupled with the algorithm of simulated annealing was used to determine the wall surface reaction constants for water treated by the methods of reverse osmosis, conventional treatment, and ozonation held at US EPA's Test and Evaluation Facility in Cincinnati, Ohio (*Rossman*, *2006*). The simulated concentrations obtained by the present approximate solution were in good agreement with the experiment-observed for lab-tested water applied by those three treatments. In the second case, the present approximate solution was also used to determine the wall surface reaction constant of the dead-end pipes in a field test conducted by SCCRWA (*Biswas et al.*, *1993*).

The high values of wall surface reaction constant in the dead-end pipes determined by the present approximate solution may imply the growth of biofilm on the wall pipe and thus lower the chlorine concentration.

In the case study of network simulation, the methodology which integrates approximate solution and Newton's method was first used to estimate the pipe wall surface reaction constant. The present model was then employed to simulate concentration distribution for a portion of the network of SCCRWA over a period of 55 hr. The concentrations determined by the present model gave good agreement with the field measurements. The simulated results by the present model gave slightly large difference at node 3 when compared with those of *Rossman et al.*'s model (*1994*). The difference between both models is mainly due to the chlorine transfer coefficient used in the simulations from bulk flow to pipe wall which is an important factor for wall decay rate. The use of the eddy diffusivity based on *Edwards et al*'s formula (1979) for the determination of concentration distribution under laminar flow condition may be not appropriate. At the present time, only few attempts were made to deal with the diffusivity for solute transport under laminar flow regime. Thus, the issue of how to determine the effective diffusivity in pipes when flow is laminar may be a practical and useful topic desired further study.

REFERENCE

Al-Jasser, A.O. "Chlorine decay in drinking-water transmission and distribution systems: Pipe service age effect", Water Res., 41, 387-396, 2007.

Biswas, P., Lu, C.S. and Clark, R.M. "A model for chlorine concentration decay in pipes", Water Res., 27(12), 1717-1724,1993.

Clark R. M., Grayman W. M., Goodrich J. A., Deininger R. A. and Hess, A. F. "Field testing distribution water quality models", J. Am. Wat. Wks Ass., 83(7), 67-75, 1991.

Clark R. M., Grayman W. M., Goodrich J. A., Males, R. M. and Hess, A. F. "Modeling contaminant propagation in drinking water distribution", J. Envir. Engrg., 119(2), 349-364,1993.

Clark R. M., *et al.* "Measuring and modeling chlorine propagation in water distribution systems", J. of Water. Resour. Plng. and Mgmt., 120(6), 67-75, 1994.

Edwards, D. K., Denny, V. E. and Mills, A. F., Transfer Processes: An Introduction to Diffusion, Convection and Radiation, 2nd ed., McGraw-Hill, New York, 1979.

Hallam, N. B., West, J. R., Forster, Powell, J.C. and Spencer, I. "The decay of chlorine associated with the pipe wall in water distribution systems", Water Res., 36(14), 3479-3488, 2002.

Jeffrey, A., Advanced Engineering Mathematics, Harcourt/Academic press, Massachusetts, 2002.

LeChevallier M. W., Cawthon, C. and Lee, R. G. "Inactivation of biofilm bacteria", Appl. Environ. Microbiol., 54, 2492-2499, 1988.

Lin, Y. C. and Yeh, H. D. "THM Species Forecast Using Optimization Method: Genetic Algorithm and Simulated Annealing", Journal of Computing in Civil Engineering ASCE, 19(3), 248-257, 2005.

Lin, Y. C. and Yeh, H. D. “Identifying Groundwater Pumping Source Information Using Optimization Approach”, Hydrological Process, 16(3), 183-188,2006.

Massabo, M., Cianci, R. and Paladino, O. “Some analytical solutions for two-dimensional convection-dispersion equation in cylindrical geometry”, Environ. Modell. Softw., 21, 681-688, 2006, doi:10.1016/j.envsoft.2004.12.003.

Munavalli, G.R. and M. S. Kumar, M. “Dynamic simulation of multicomponent reaction transport in water distribution systems”, Water Res., 38, 1971-1988, 2004a.

Munavalli, G.R. and M. S. Kumar, M. “Modified Lagrangian method for modeling water quality in distribution systems”, Water Res., 38, 2973-2988, 2004b.

Munavalli, G.R. and M. S. Kumar, M. “Autocalibration of a water distribution model for water quality parameters using GA”, J. AWWA., 98(9), 109-123, 2006.

Oberhettinger, F. and Badii, L., Tables of Laplace Transforms, Spring-Verlag Berlin Heidelberg, New York, 1973.

Ozdemir, O. N. and Ger, A. M. “Realistic numerical simulation of chlorine decay in pipes”, Wat. Res., 32(11), 3307-3312, 1998.

Ozdemir, O. N. and Ger, A. M. “Unsteady 2-D chorine transport in water supply pipe”, Wat. Res., 33(17), 3637-3645, 1999.

Rossman, L. A. and Boulos, P. F. “Discrete volume - element method for network water - quality models”, J. of Water. Resour. Plng. and Mgmt., 119(5), 505-517, 1993.

Rossman, L.A., Clark, R.M. and Grayman, W.M. “Modeling chlorine residuals in drinking-water distribution systems”, J. Environ. Eng., 120(4), 803–820, 1994.

Rossman, L. A. and Boulos, P. F. “Altman T. Numerical methods for water quality in distribution system: A comparison”, J. of Water. Resour. Plng. and Mgmt., 122(2), 137-146, 1996.

Rossman, L. A., EPANET 2 Users Manual, US Environmental Protection Agency, Cincinnati, 2000.

Rossman, L. A. “The effect of advanced treatment on chlorine decay in metallic pipes”, Wat. Res., 40, 2493-2502, 2006.

Tchobanoglous, G. and Schroeder, E.D., Water Quality, Addison-Wesley Publishing Company, 1987.

Vasconcelos, J. J., Rossman, L. A., Grayman, W. M. and Boulos, P. F. “Kinetics of chlorine decay”, J. AWWA., 89(7), 54-65, 1997.

Wood, D. J., KYPIPEF User’s Manual, University of Kentucky, Lexington, KY, 1986.

Yang, S.Y. and Yeh, H. D. “Solution for flow rates across the wellbore in a two-zone confined aquifer”, Journal of Hydraulic Engineering ASCE, 128(2), 175-183, 2002.

Yeh, G.T., Computational Subsurface Hydrology, Kluwer Academic Publisher, USA, 2000.

Yeh, H. D. “Theis’ solution by nonlinear least-squares and finite-difference Newton’s method”, Ground Water, 25, 710-715, 1987.

Yeh, H. D. and Chen, Y. J. “Determination of Skin and Aquifer Parameters for a Slug Test with Wellbore-skin Effect”, Journal of Hydrology, 342, 283-294, 2007, doi:10.1016/j.jhydrol.2007.05.029.

Yeh, H. D., Lin, Y. C. and Huang, Y. C. “Parameter Identification for Leaky Aquifers Using Global Optimization Methods”, Hydrological Processes, 21, 862-872, 2007a, doi:10.1002/hyp.6274.

Yeh, H. D., Chang, T. H. and Lin, Y. C. “Groundwater Contaminant Source Identification by a Hybrid Heuristic Approach”, Water Resources Research, 43, 2007b, doi:10.1029/2005WR004731.

APPENDIX A: DERIVATION OF EQUATION (17)

The Laplace transform for the concentration, $C(R, X, T)$ can be expressed

$$\mathrm{L}\left[C\left(R,X,T\right)\right]=\overline{C}\left(R,X,s\right) \tag{A1}$$

where s is the Laplace parameter. After taking the Laplace transform subject to the initial condition, the transport equation, Eq. (7), becomes

$$\frac{\partial\overline{C}}{\partial X}=\frac{1}{P_{\mathrm{L}}}\frac{\partial^2\overline{C}}{\partial X^2}+\frac{D}{R}\frac{\partial}{\partial R}\left(R\frac{\partial\overline{C}}{\partial R}\right)-\left(K+s\right)\overline{C}+\hat{\beta}\exp(-\hat{\alpha}X) \tag{A2}$$

The Laplace transforms of the boundary conditions Eqs. (9) – (12) are

$$\overline{C}\left(R,0,s\right)=\frac{\tilde{\beta}}{s+\tilde{\alpha}} \tag{A3}$$

$$\overline{C}\left(R,\infty,s\right)=0 \tag{A4}$$

$$\left.\frac{\partial\overline{C}\left(0,X,s\right)}{\partial R}\right|_{R=0}=0 \tag{A5}$$

$$\left.\frac{\partial\overline{C}\left(R,X,s\right)}{\partial R}\right|_{R=1}=-W\overline{C}\left(1,X,s\right) \tag{A6}$$

Note that the Sturm-Liouville boundary value problem (S-L BVP) is described as (*Jeffrey, 2002, p. 517*)

$$\frac{1}{R}\frac{d}{dR}\left(R\frac{dF}{dR}\right)=\xi F \tag{A7}$$

The associated boundary conditions are

$$\left.\frac{dF}{dR}\right|_{R=0}=0 \tag{A8}$$

$$\left.\frac{dF}{dR}\right|_{R=1}=-WF \tag{A9}$$

where F and ξ are the dependent variable of S-L BVP and a parameter respectively. The second RHS term of Eq. (A2) along with the associated boundary condition can be considered

as a S-L BVP. The eigenfunction of the S-L BVP is $J_0(\lambda_n R)$ given in *Biswas et al.* (*1993*) where the eigenvalue λ_n is the *n*th root of the eigenfunction, $\lambda_n J_1(\lambda_n) = W J_0(\lambda_n)$ and equal to $\xi^{0.5}$. A function can be represented by the generalized Fourier series called the eigenfunction expansion (*Jeffrey*, *2002*). Thus, the function $\bar{C}$ and the second RHS term of Eq. (A2) can be expanded using the zero order Bessel function, $J_0(\lambda_n R)$, as, respectively

$$\bar{C}(R, X, s) = \sum_{n=1}^{\infty} \bar{X}_n(X, s) J_0(\lambda_n R) \tag{A10}$$

and

$$\hat{\beta} \exp(-\hat{\alpha}) = \hat{\beta} \exp(-\hat{\alpha}) \sum_{n=1}^{\infty} E_n J_0(\lambda_n R) \tag{A11}$$

where E_n is (*Biswas et al.*, *1993*)

$$E_n = \frac{\langle 1, J_0(\lambda_n R) \rangle}{\| J_0(\lambda_n R) \|^2} \tag{A12}$$

Based on *Biswas et al.* (*1993*), E_n can be written as $2J_0(\lambda_n) / \lambda_n \left[J_0^2(\lambda_n) + J_1^2(\lambda_n) \right]$. Substituting Eqs. (A10) and (A11) into Eq. (A2), the second RHS term of Eq. (A2) can be expressed based on Eq. (A7) as

$$\frac{D}{R} \frac{\partial}{\partial R} \left(R \frac{\partial \bar{C}}{\partial R} \right) = \sum_{n=1}^{\infty} D \lambda_n^2 \bar{X}_n J(\lambda_n R) \tag{A13}$$

and, thus, Eq. (A2) becomes

$$\sum_{n=1}^{\infty} \left\{ -\frac{1}{P_L} \bar{X}_n'' + \bar{X}_n' + \Gamma_n \bar{X}_n \right\} J(\lambda_n R) = \hat{\beta} \exp(-\hat{\alpha}) \sum_{n=1}^{\infty} E_n J(\lambda_n R) \tag{A14}$$

where Γ_n represents $(K + \lambda_n^2 D)$. The eigenfunction expansions for the boundary conditions of Eqs. (A3) and (A4) are respectively

$$\sum_{n=1}^{\infty} \bar{X}_n(0, s) J_0(\lambda_n R) = \frac{\tilde{\beta}}{s + \tilde{\alpha}} \tag{A15}$$

$$\sum_{n=1}^{\infty} \bar{X}_n(\infty, s) J_0(\lambda_n R) = 0 \tag{A16}$$

Based on the formula of generalized Fourier series (*Jeffrey*, *2002*), the $\bar{X}_{\mathrm{n}}$'s in Eqs. (A15) and (A16) can be respectively obtained as

$$\bar{X}_{\mathrm{n}}\left(0,s\right)=E_{\mathrm{n}}\frac{\tilde{\beta}}{s+\tilde{\alpha}} \tag{A17}$$

$$\bar{X}_{\mathrm{n}}\left(\infty,s\right)=0 \tag{A18}$$

As crossing out the Bessel function on both sides of Eq. (A14), an ordinary differential equation can be found as

$$-\frac{1}{P_{\mathrm{L}}}\bar{X}_{\mathrm{n}}''+\bar{X}_{\mathrm{n}}'+\Gamma_{\mathrm{n}}\bar{X}_{\mathrm{n}}=E_{\mathrm{n}}\hat{\beta}\exp(-\hat{\alpha}) \tag{A19}$$

The Eq. (A20) subject to boundary conditions Eqs. (A17) and (A18) can be easily solved as

$$\begin{aligned}\bar{X}_{\mathrm{n}}\left(X,s\right)=&\frac{2J_{1}\left(\lambda_{\mathrm{n}}\right)}{\lambda_{n}\left[J_{1}^{2}\left(\lambda_{\mathrm{n}}\right)+J_{0}^{2}\left(\lambda_{\mathrm{n}}\right)\right]}\\&\left\{\left[\frac{\tilde{\beta}}{\left(s+\tilde{\alpha}\right)}+\frac{\hat{\beta}}{\left(\hat{\alpha}^{2}/P_{\mathrm{L}}+\hat{\alpha}-\Gamma_{\mathrm{n}}-s\right)}\right]\exp\left[\frac{P_{\mathrm{L}}X}{2}\left(1-\sqrt{1+\frac{4}{P_{\mathrm{L}}}\left(\Gamma_{\mathrm{n}}+s\right)}\right)\right]\right.\\&\left.-\frac{\hat{\beta}}{\left(\hat{\alpha}^{2}/P_{\mathrm{L}}+\hat{\alpha}-\Gamma_{\mathrm{n}}-s\right)}\exp\left(-\hat{\alpha}X\right)\right\}\end{aligned} \tag{A20}$$

Based on Eq. (A10), the Laplace-domain solution for unsteady 2-D CTE is developed as Eq. (15). The inverse Laplace transforms can be obtained with the application of convolution theorem to the first and second terms on the RHS of Eq. (A20). The first RHS term of Eq. (A20) can be expressed as

$$\begin{aligned}&\mathrm{L}^{-1}\left\{\frac{\tilde{\beta}}{\left(s+\tilde{\alpha}\right)}\exp\left[\frac{P_{\mathrm{L}}X}{2}\left(1-\sqrt{1+\frac{4}{P_{\mathrm{L}}}\left(\Gamma_{\mathrm{n}}+s\right)}\right)\right]\right\}\\&=\int_{0}^{T}\mathrm{L}^{-1}\left[\frac{\tilde{\beta}}{\left(s+\tilde{\alpha}\right)}\right]\Bigg|_{T=T-\delta}\mathrm{L}^{-1}\left\{\exp\left[\frac{P_{\mathrm{L}}X}{2}\left(1-\sqrt{1+\frac{4}{P_{\mathrm{L}}}\left(\Gamma_{\mathrm{n}}+s\right)}\right)\right]\right\}\Bigg|_{T=\delta}\mathrm{d}\delta\end{aligned} \tag{A21}$$

Applying the inverse Laplace transform (*Oberhettinger and Badii*, *1973*), we get

$$\mathrm{L}^{-1}\left[\frac{\tilde{\beta}}{\left(s+\tilde{\alpha}\right)}\right]=\tilde{\beta}\exp\left(-\tilde{\alpha}T\right) \tag{A22}$$

and

$$\mathrm{L}^{-1}\left\{\exp\left[\frac{P_{\mathrm{L}}X}{2}\left(1-\sqrt{1+\frac{4}{P_{\mathrm{L}}}\left(\Gamma_{\mathrm{n}}+s\right)}\right)\right]\right\}=\frac{x}{2}\sqrt{\frac{P_{\mathrm{L}}}{\pi T^{3}}}\exp\left[-\frac{P_{\mathrm{L}}X^{2}}{4T}-T\left(\frac{P_{\mathrm{L}}}{4}+\Gamma_{\mathrm{n}}\right)\right] \tag{A23}$$

Thus, Eq. (A21) becomes

$$\begin{aligned}&\mathrm{L}^{-1}\left\{\frac{\tilde{\beta}}{\left(s+\tilde{\alpha}\right)}\exp\left[\frac{P_{\mathrm{L}}X}{2}\left(1-\sqrt{1+\frac{4}{P_{\mathrm{L}}}\left(\Gamma_{\mathrm{n}}+s\right)}\right)\right]\right\}\\&=\frac{x}{2}\sqrt{\frac{P_{\mathrm{L}}}{\pi}}\tilde{\beta}\exp\left(-\tilde{\alpha}T\right)\int_{0}^{T}\tau^{-\frac{3}{2}}\exp\left[-\frac{P_{\mathrm{L}}X^{2}}{4\tau}-\tau\left(-\tilde{\alpha}+\frac{P_{\mathrm{L}}}{4}+\Gamma_{\mathrm{n}}\right)\right]\,\mathrm{d}\tau\end{aligned} \tag{A24}$$

Based on the integral result given in *Massabo et al.* (*2006*, Eq. (2.31)), Eq. (A24) becomes

$$\mathrm{L}^{-1}\left\{\frac{\tilde{\beta}}{\left(s+\tilde{\alpha}\right)}\exp\left[\frac{P_{\mathrm{L}}X}{2}\left(1-\sqrt{1+\frac{4}{P_{\mathrm{L}}}\left(\Gamma_{\mathrm{n}}+s\right)}\right)\right]\right\}=A(X,T) \tag{A25}$$

where $A(X, T)$ is defined in Eq. (18). Similarly, the inverse Laplace transform of the second RHS term of Eq. (A20) can be obtained as

$$\mathrm{L}^{-1}\left[\frac{\hat{\beta}}{\left(\hat{\alpha}^{2}/P_{\mathrm{L}}+\hat{\alpha}-\Gamma_{\mathrm{n}}-s\right)}\exp\left[\frac{P_{\mathrm{L}}X}{2}\left(1-\sqrt{1+\frac{4}{P_{\mathrm{L}}}\left(\Gamma_{\mathrm{n}}+s\right)}\right)\right]\right]=B(X,T) \tag{A26}$$

where $B(X, T)$ is defined in Eq. (19). The inverse Laplace transform of the third RHS term of Eq. (A20) is

$$\mathrm{L}^{-1}\left[\frac{\hat{\beta}}{\left(\hat{\alpha}^{2}/P_{\mathrm{L}}+\hat{\alpha}-\Gamma_{\mathrm{n}}-s\right)}\exp\left(-\hat{\alpha}X\right)\right]=\hat{\beta}\exp\left[\left(\hat{\alpha}/P_{\mathrm{L}}+\hat{\alpha}-\Gamma_{\mathrm{n}}\right)T\right]\exp\left(-\hat{\alpha}X\right) \tag{A27}$$

Based on Eq, (15) and Eqs. (A25) - (A27), the analytical solution of unsteady 2-D CTE under turbulent flow condition is

$$\begin{aligned}C\left(R,X,T\right)=\sum_{n=1}^{\infty}\frac{2J_{1}\left(\lambda_{\mathrm{n}}\right)J_{0}\left(\lambda_{\mathrm{n}}R\right)}{\lambda_{\mathrm{n}}\left[J_{1}^{2}\left(\lambda_{\mathrm{n}}\right)+J_{0}^{2}\left(\lambda_{\mathrm{n}}\right)\right]}\times\Big\{&\tilde{\beta}\exp(-\tilde{\alpha}T)A(X,T)\\&-\hat{\beta}\exp\left[\left(\hat{\alpha}/P_{\mathrm{L}}+\hat{\alpha}-\Gamma_{\mathrm{n}}\right)T\right]\left[B(X,T)-\exp(-\hat{\alpha}X)\right]\Big\}\end{aligned} \tag{A28}$$

The cup-mixing average concentration can now be expressed as

$$C_{\mathrm{av}}=\left(\int_{0}^{1}C(R,X,T)\pi R\;\mathrm{d}R\right)\left(\frac{1}{\pi R^{2}}\right) \tag{A29}$$

Substituting $C(R, X, T)$ into equation (A29), Eq. (17) can be found after performing the integration of (A29).

Table 1. The values of λ_1 at different W

W	Newton's method	Approximate method	Relative error (%)
0.001	0.04472	0.04471	-0.02
0.01	0.01412	0.01411	-0.07
0.1	0.44168	0.43644	-1.19
0.5	0.94077	0.89443	-4.93

Table 2. The values of k_d and w_d for three sorts of lab-tested water

Treatment	k_d (1/s)	w_d (m/s)		
		First-order reaction model (*Rossman*, *2006*)	Present approximate solution	*Biswas et al.*'s approximate solution (*1993*)
RO	8.10×10^{-8}	4.66×10^{-7}	4.50×10^{-7}	4.20×10^{-7}
CON	1.09×10^{-7}	6.73×10^{-7}	6.52×10^{-7}	6.43×10^{-7}
O_3	5.56×10^{-7}	1.30×10^{-6}	1.33×10^{-6}	1.53×10^{-6}

Table 3. Chlorine concentrations at the inlet and outlet of various segments

Pipe in segment	Chlorine concentration at segment			
	C_{in} (*Biswas et al., 1993*)	C_{out} (*Biswas et al., 1993*)	C_{out}/C_{in}	C_{av}/C_{in}
1,3	1.08	1.00	0.926	0.926
7, 9, 11	1.00	0.98	0.980	0.975
7, 8, 10	1.00	0.32	0.320	0.319
7, 9, 11 to 15, 26 to 28	1.00	0.94	0.940	0.940
12, 13, 16, 21	0.98	0.16	0.163	0.161
12 to 15, 26 to 28	0.98	0.94	0.959	0.964

Table 4. Parameters for different pipes in the network

Pipe	Length (m)	Radius (m)	Flow velocity (m/s)	Diffusion coefficient (m^2/s)	w_d (m/s)
1	731.5	0.152	0.546	1.02×10^{-03}	3.47×10^{-07}
3	396.2	0.102	0.195	2.45×10^{-04}	1.24×10^{-06}
7	822.9	0.152	0.512	9.60×10^{-04}	3.47×10^{-07}
8	365.8	0.152	0.014	2.62×10^{-05}	3.47×10^{-07}
9	121.9	0.152	0.494	9.26×10^{-04}	3.47×10^{-07}
10	304.8	0.102	0.014	$1.76\times10\text{-}^{05}$	1.64×10^{-06}
11	213.4	0.152	0.485	9.09×10^{-04}	3.47×10^{-07}
12	579.1	0.152	0.457	8.56×10^{-04}	3.47×10^{-07}
13	182.9	0.152	0.445	8.34×10^{-04}	3.47×10^{-07}
14	121.9	0.152	0.372	6.97×10^{-04}	3.47×10^{-07}
15	91.4	0.152	0.329	6.17×10^{-04}	3.47×10^{-07}
16	457.2	0.102	0.168	2.11×10^{-04}	3.47×10^{-07}
21	426.7	0.102	0.049	6.16×10^{-05}	1.01×10^{-05}
26	76.2	0.152	0.338	6.33×10^{-04}	3.47×10^{-07}
27	182.9	0.152	0.329	6.17×10^{-04}	3.47×10^{-07}
28	91.4	0.152	0.323	6.05×10^{-04}	3.47×10^{-07}

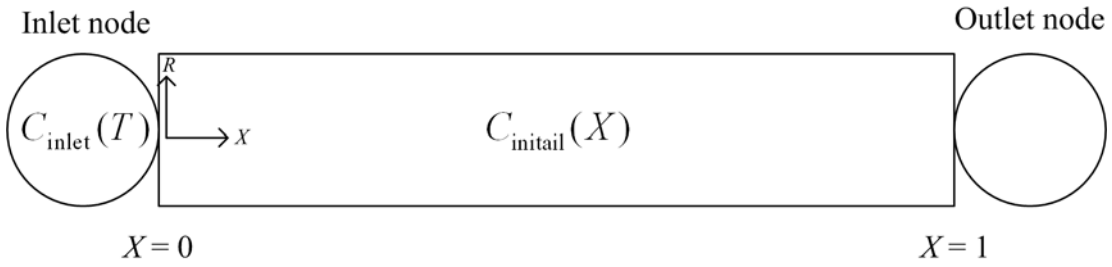

Figure 1. A dimensionless control volume with initial and inlet conditions

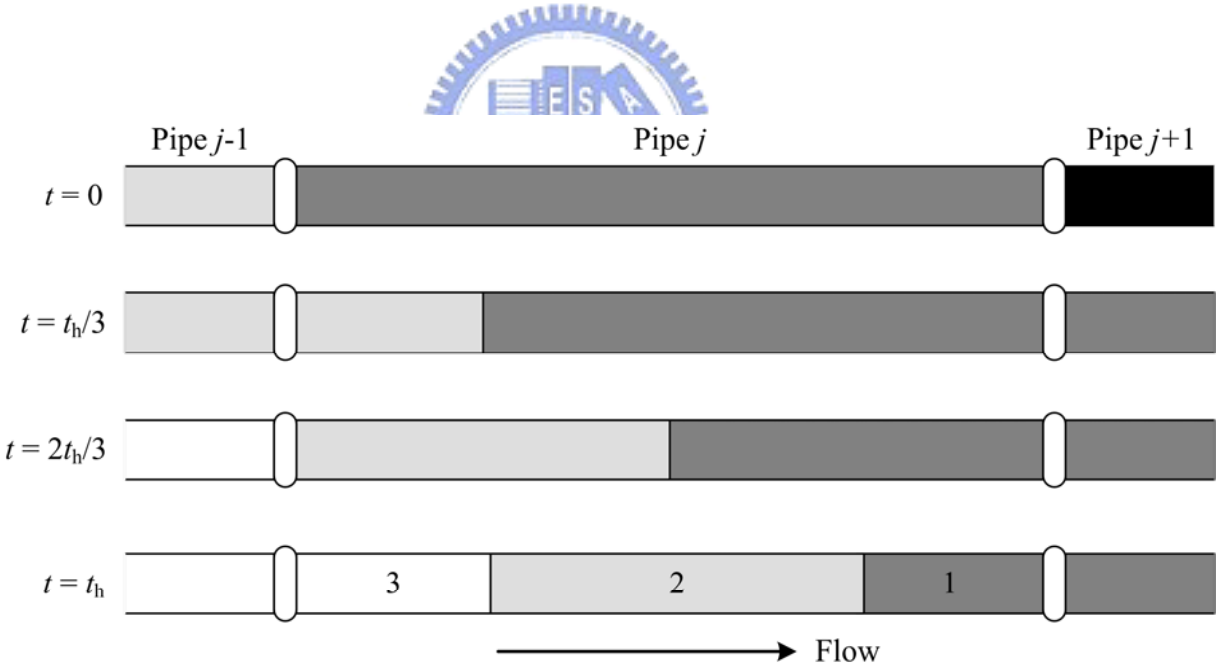

Figure 2. Example of a network for chlorine concentration calculation.

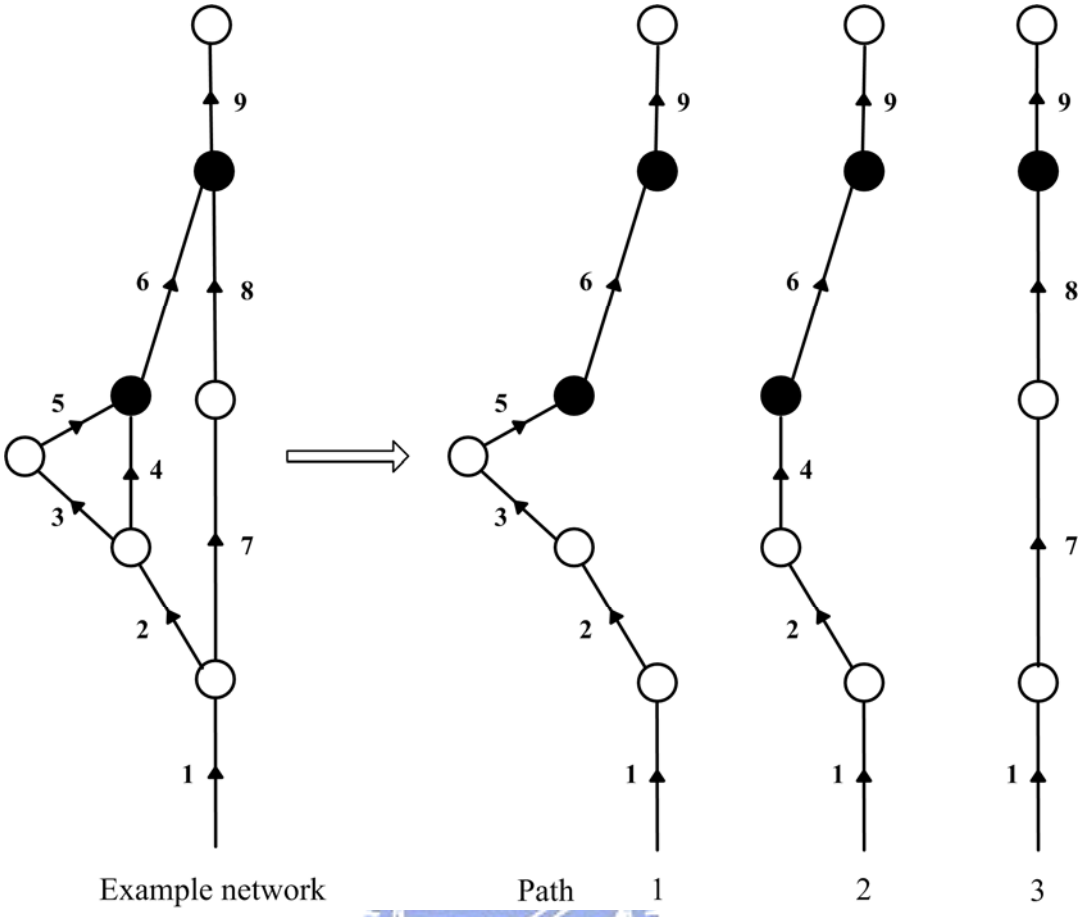

Figure 3. Example of network for chlorine calculation using analytical model.

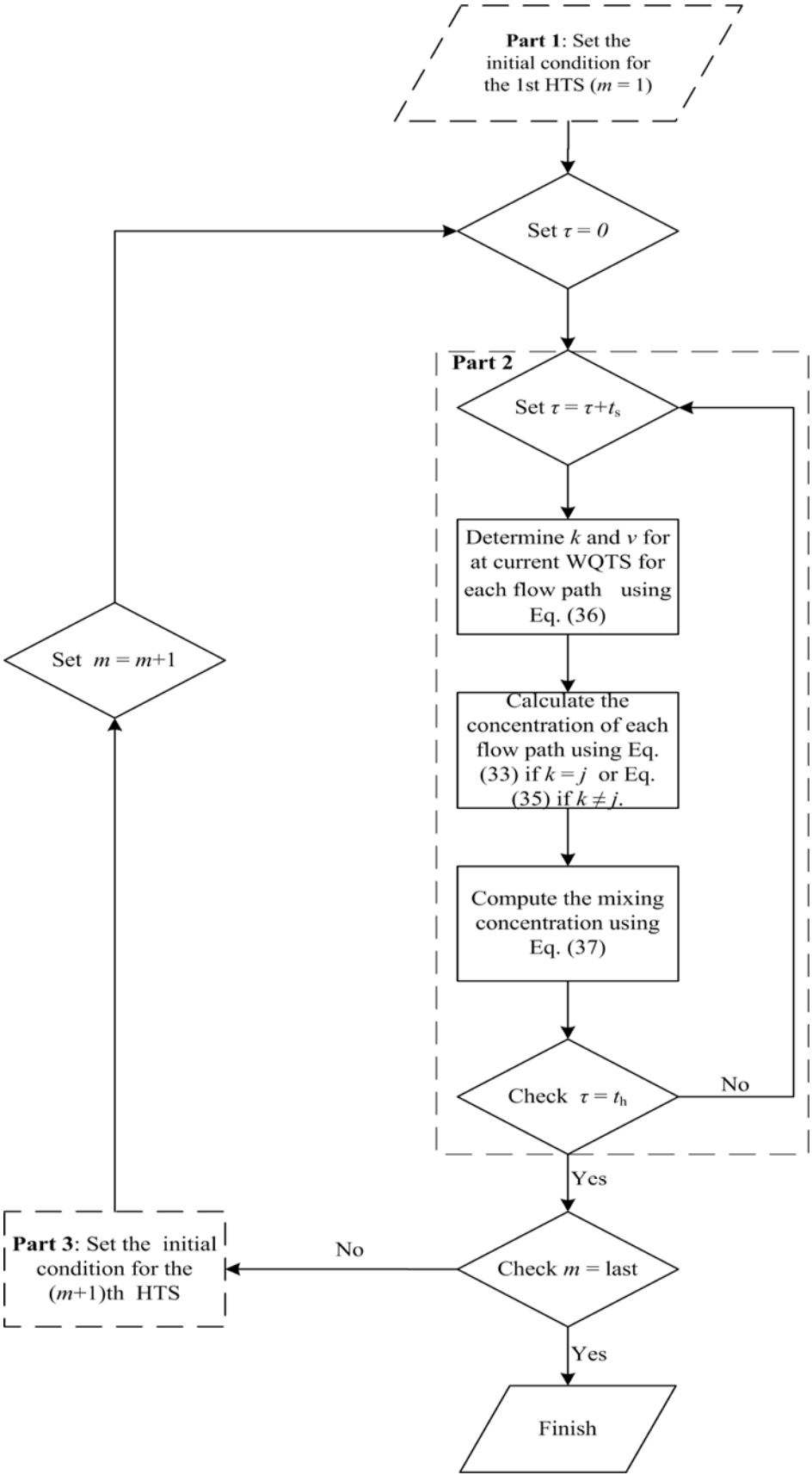

Figure 4. Flowchart of the methodology analytical model.

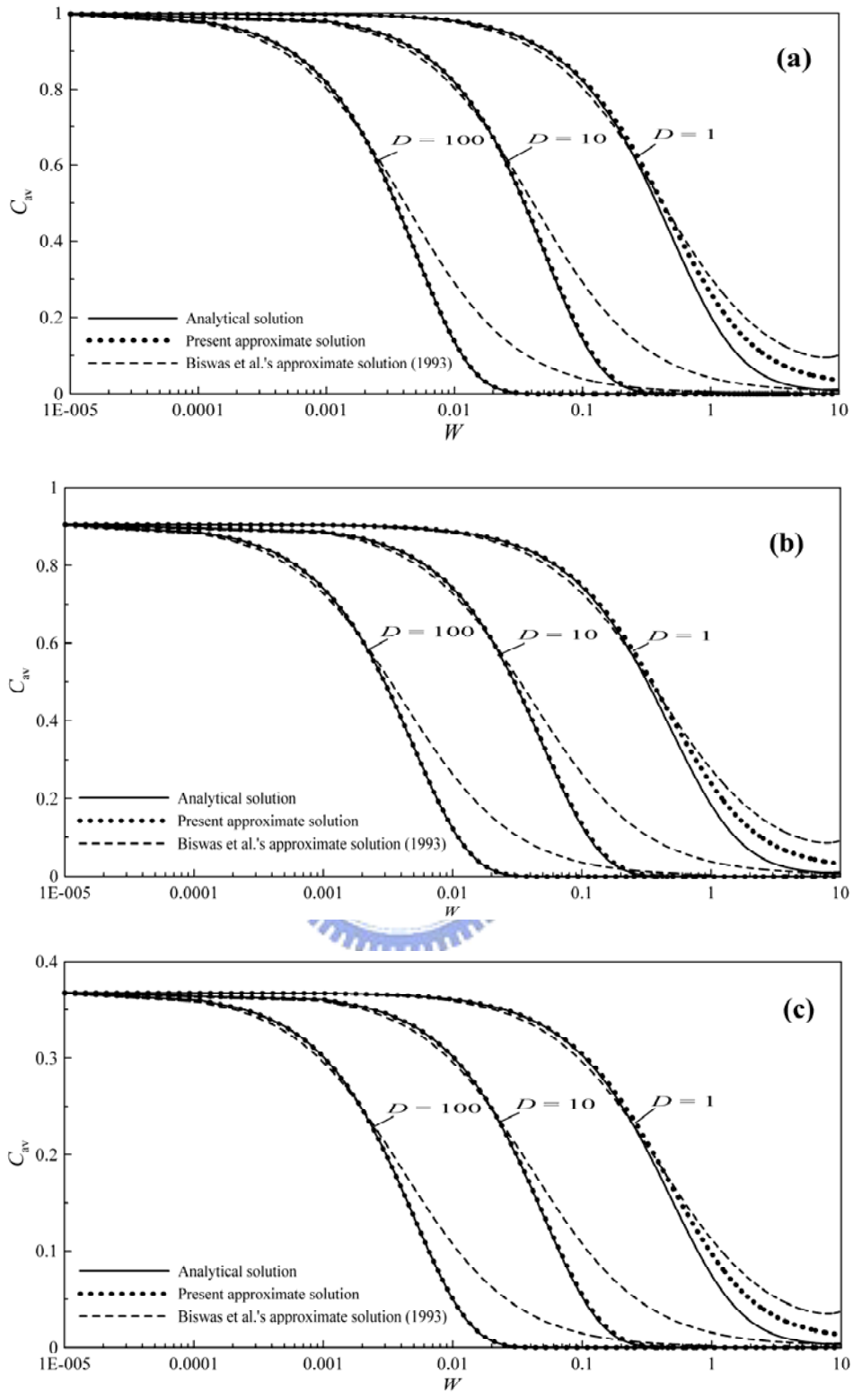

Figure 5. Computed values of analytical solution, presented approximate solution and *Biswas et al.*'s approximate solution (*1993*) at the outlet of pipe against W at K = (a) 0.001, (b) 0.1, (c) 1.

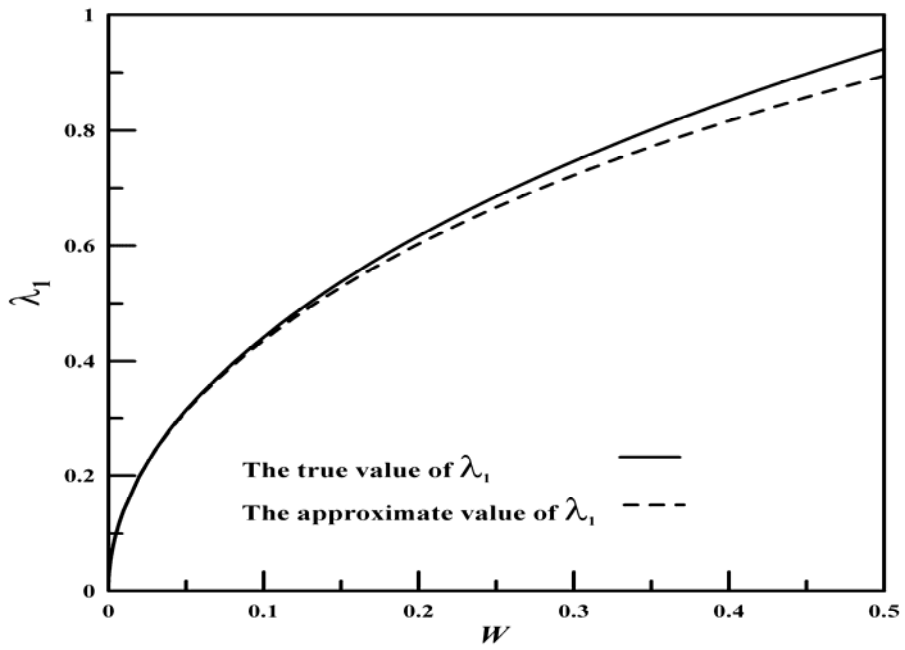

Figure 6. The λ_1 against W for the true values and approximate values.

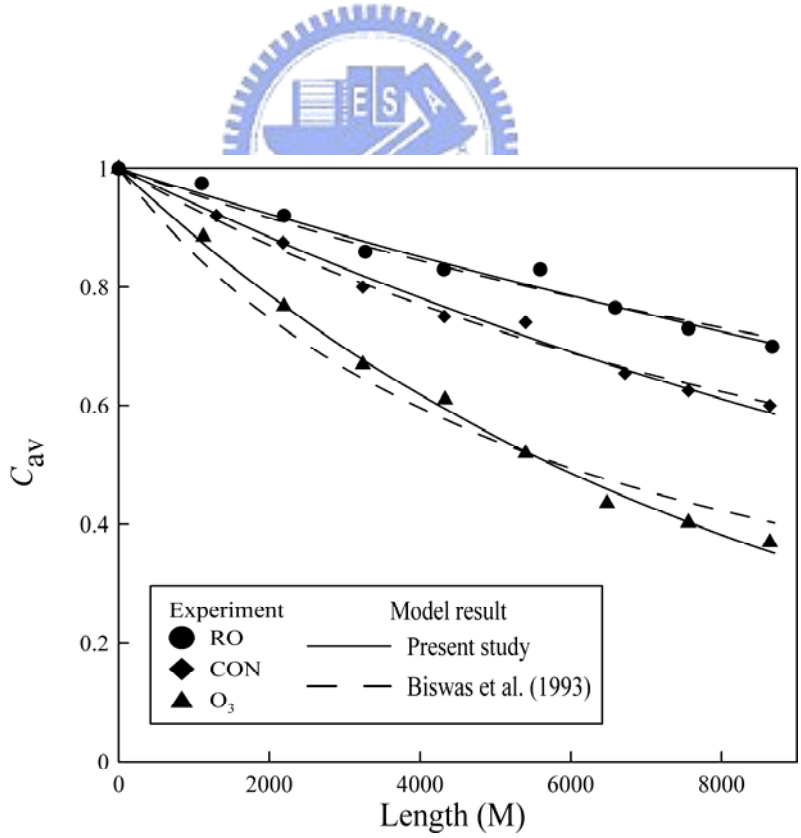

Figure 7. The experiment-observed data (*Rossman*, *2006*) and simulated results of the present approximate solution and *Biswas et al.*'s approximate solution (*1993*) for three sorts of lab-tested water.

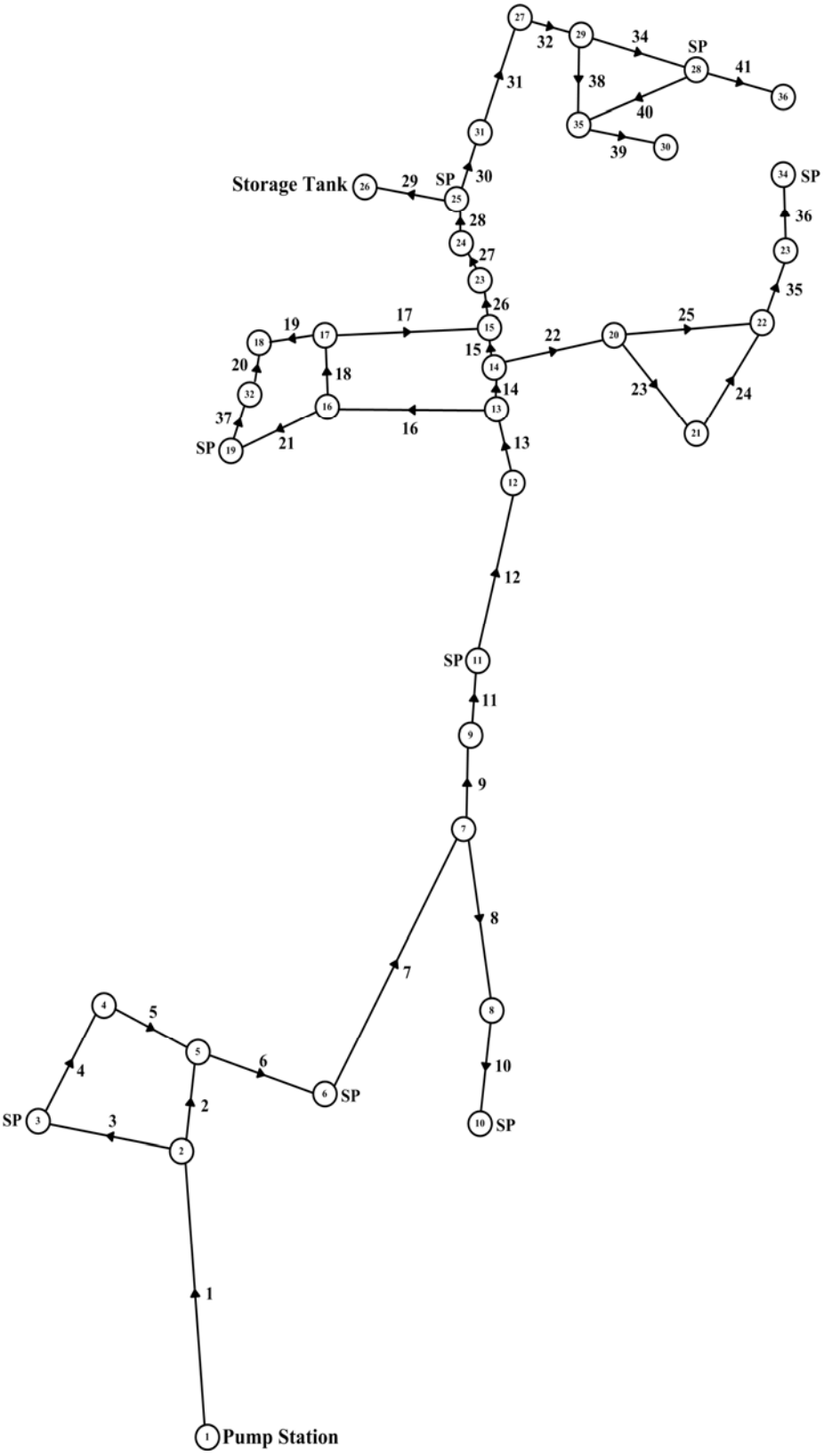

Figure 8. Schematic of water network at New Haven, Connecticut. The arrows represent the flow direction at the 3rd HTS and "SP" is denoted as the sampling node.

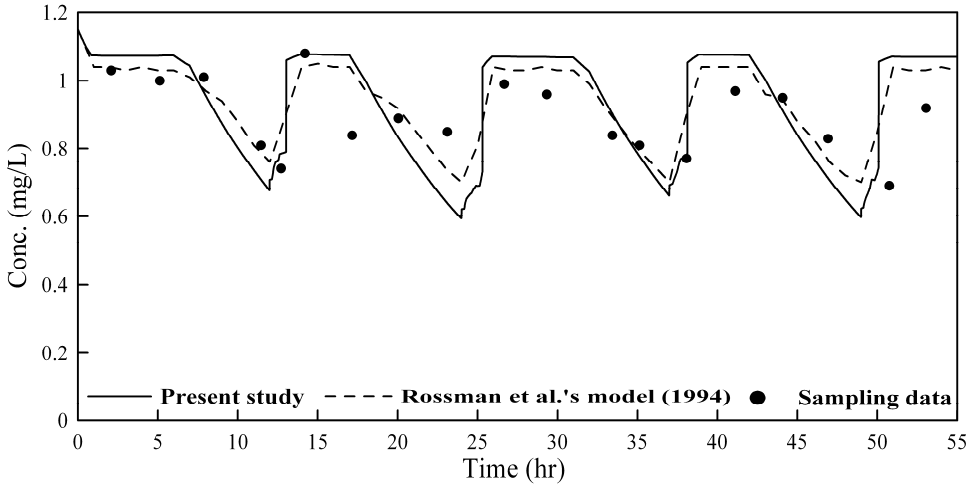
Conc. (mg/L)
Time (hr)
Present study
Rossman et al.'s model (1994)
Sampling data

(a)

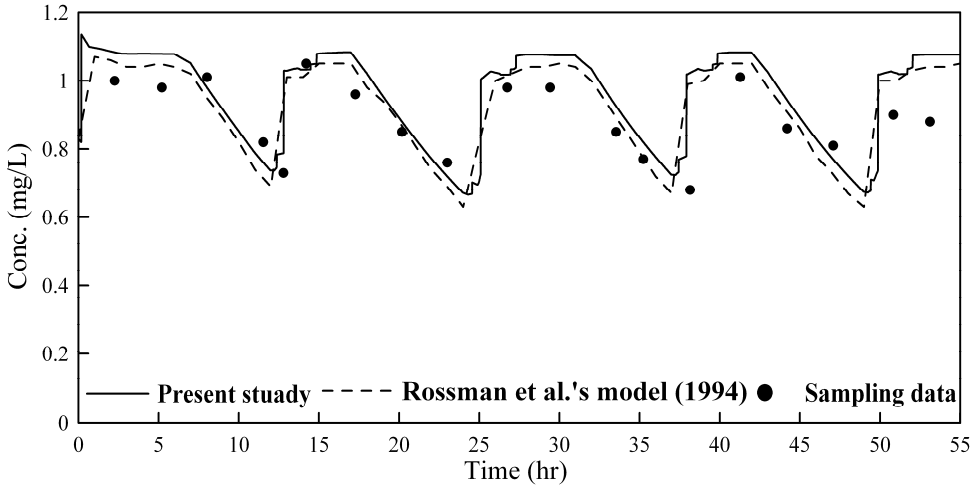
Conc. (mg/L)
Time (hr)
Present stuady
Rossman et al.'s model (1994)
Sampling data

(b)

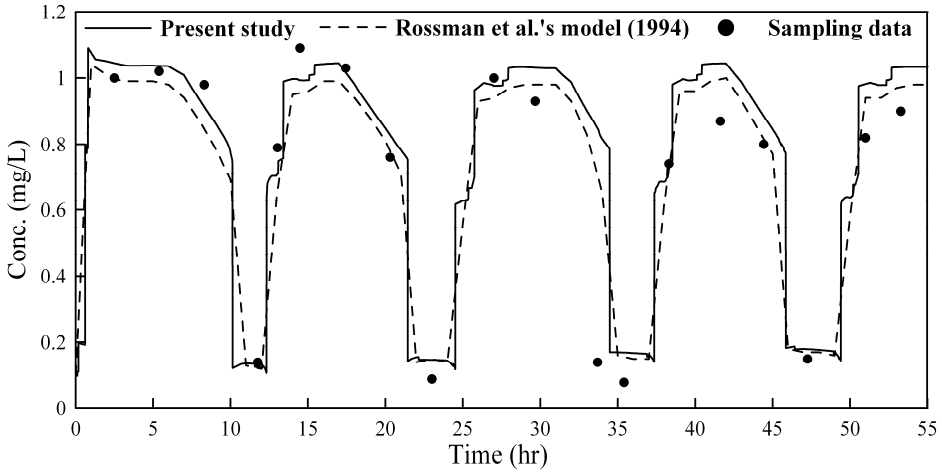
Conc. (mg/L)
Time (hr)
Present study
Rossman et al.'s model (1994)
Sampling data

(c)

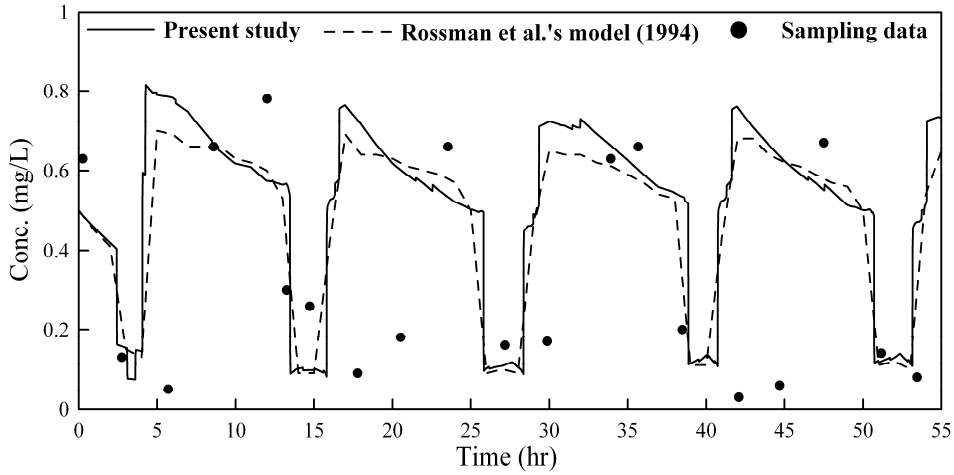

(d)

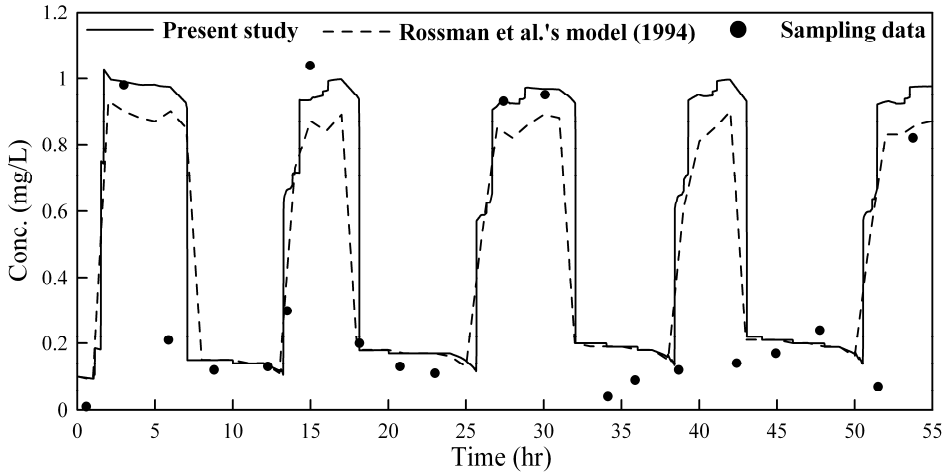

(e)

Figure 9. The simulated concentration based on present model and *Rossman et al.*'s model (*1994*) comparing with sampling data against time at node (a) 3, (b) 6, (c) 11 (d) 19, (e) 25.

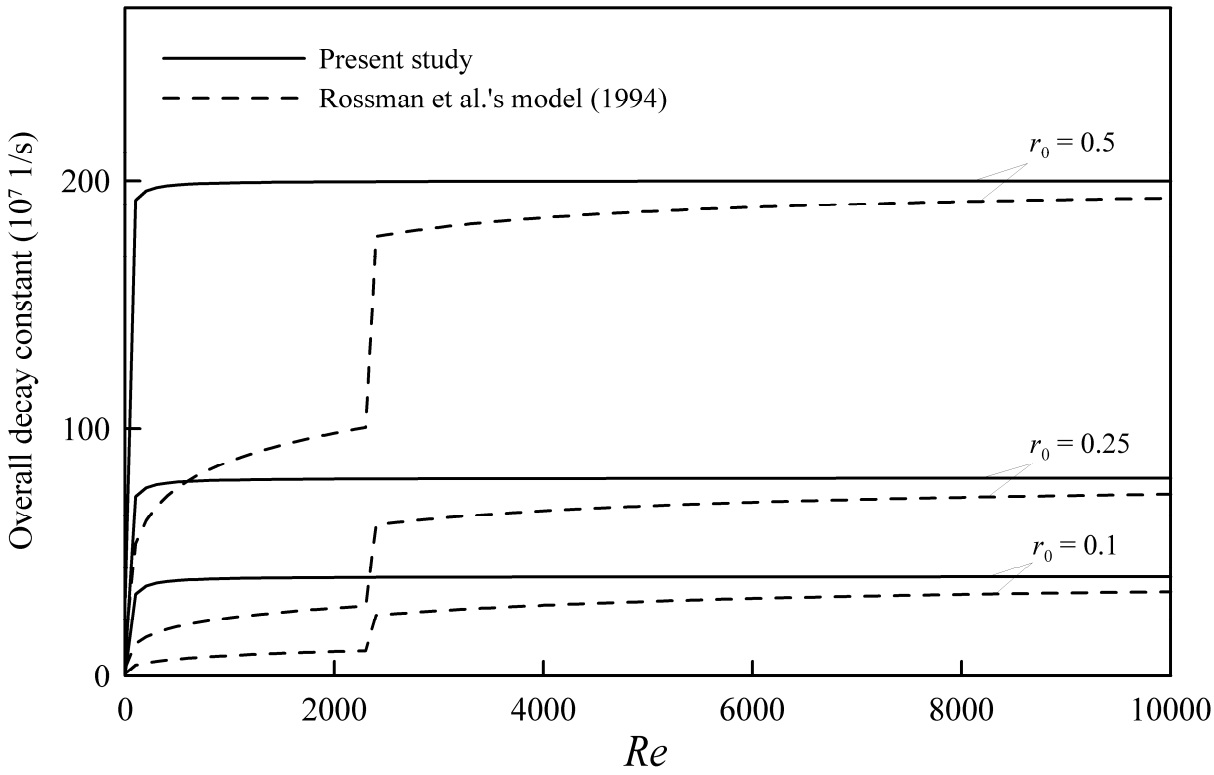

Figure 10. The curves of the overall decay constant computed based on the present model and the *Rossman et al.*'s model (*1994*) against *Re* at $w_d = 1\times10^{-6}$ (m/s) and $k_d = 0$ in pipe 3.

個人資料

姓名：溫士賓

生日：民國73年5月2日

出生地：新竹市

電話：03-5207943

住址：新竹市明湖路604巷7號

學歷：民國95年畢業於國立中興大學環境工程學系

民國97年畢業於國立交通大學環境工程研究所